Transition drivers and crisis signaling in stock markets

Spelta, Alessandro and Pecora, Nicolò and Flori, Andrea and Pammolli, Fabio

Center for Analysis, Decisions, and Society (CADS) - Human Technopole, Milano, Italy, Catholic University - Department of Economics and Social Sciences, Piacenza, Italy, Politecnico di Milano, Department of Management, Economics and Industrial Engineering, Italy, Politecnico di Milano, Department of Management, Economics and Industrial Engineering, Italy

23 July 2018

Transition drivers and crisis signaling in stock markets

Alessandro Spelta[*a,b], Nicolò Pecora [†c], Andrea Flori[‡d], and Fabio Pammolli [§a,d]

[a]Center for Analysis, Decisions, and Society (CADS) - Human Technopole, Milano, Italy

[b]Complexity Lab in Economics, Milano, Italy

[c]Catholic University - Department of Economics and Social Sciences, Piacenza

[d]Politecnico di Milano, Department of Management, Economics and Industrial Engineering

Abstract

The present paper introduces an up-to-date methodology to detect Early Warning Signals of critical transitions, that manifest when distress stages in financial markets are about to take place. As a first step, we demonstrate that a high-dimensional dynamical system can be formulated in a simpler form but in an abstract phase space. Then we detect its approaching towards a critical transition by means of a set of observable variables that exhibit some particular statistical features. We name these variables the Leading Temporal Module. The impactful change in the properties of this group reflects the transition of the system from a normal to a distress state. Starting from these observations we develop an early warning indicator for determining the proximity of a financial crisis. The proposed measure is model free and the application to three different stock markets, together with the comparison with alternative systemic risk measures, highlights the usefulness in signaling upcoming distress phases. Computational results establish that the methodology we propose is effective and it may constitute a relevant decision support mechanism for macro prudential policies.

Keywords: Financial Crisis, Early Warning Signals, Critical Transition, Leading Temporal Module

JEL codes: G01, G17, C02, C53, E37

[*]Email: alessandro.spelta@htechnopole.it

[†]Email: nicolo.pecora@unicatt.it

[‡]Email: andrea.flori@polimi.it

[§]Email: fabio.pammolli@polimi.it

1 Introduction

In the aftermath of the 2008-09 global financial crisis, the effort in discovering the underlying instabilities of economic systems has produced a vast theoretical and empirical literature on Early Warning Signals (EWSs). The practical implementation of tools targeting systemic risk, indeed, requires the identification of EWSs that could provide a ground for the activation of macro-prudential policies as conveyed in the notes on Macroprudential policy frameworks, produced by the Financial Stability Board (FSB), the International Monetary Fund (IMF) and the Bank for International Settlements (BIS) in February 2011 (see FSB (2011); IMF (2011); Rhu et al. (2011)).

Several works have been tackling the development of EWSs that could provide to policymakers and market participants warnings on an upcoming financial distress (for a review of the main EWSs applied in economics and finance see Bisias et al. (2012)). Most of these methods, however, have some restrictions because they assume that their underlying models remain valid even when sudden changes occur. To put it differently, they postulate precise functional forms for modelling the motion of the relevant variables. Nevertheless, these assumptions are too strong because sudden changes, such as financial crunches, might modify the qualitative and quantitative characteristics of the underlying economic system. A crisis is, by definition, a break in the law of motion describing the system, such that the rules governing the dynamic of the variables prior to the crisis do not apply anymore during (and after) the catastrophic event. Graph-theoretical tools are helpful in this circumstance to reveal how the character and the progress of financial relationships induce distinguishable patterns of structural modifications in the economic variables. The departures from a standard configuration due to a crisis could indeed be examined by using topological methods revealing the reduced decomposability of the underlying system (see Simon and Ando (1961); Ando and Fisher (1963); Simon (1996); Courtois (2014)). The definition of a crisis as a ripple effect, in which a financial distress spreads between financial institutions until it strikes the entire system, agrees with the definition provided by Simon (1996) of a non-decomposable system. The latter refers to a system in which every part is virtually related with all other parts while, by contrast, a decomposable system is one in which all (or most of) the relationships take place within the subsystems and little or none among the subsystems.

A purely topological analysis is, however, a static descriptor of the interactions occurring at a

certain time. Forecasting, however, needs a dynamic approach. In this work, a novel model-free (network-based) method is presented to detect EWSs of financial crisis, merging static and dynamic analysis. We theoretically establish that a set of stocks, that we name the Leading Temporal Module (LTM), can serve as a general EWS, indicating an imminent financial crisis. The dynamic of the LTM can be linked to the degree of decomposability of the Jacobian matrix of an unobserved system describing the stock returns dynamics (see Simon and Ando (1961); Ando and Fisher (1963); Simon (1996); Courtois (2014)). The alteration in the statistical features of this group is indeed the empirical reflection of a reduced level of decomposability of such a matrix. This means that, even without specifying a functional form for the variables law of motion, we can detect a signal which mirrors a transition in the variables evolution in different dynamical phases.

Specifically, we employ the theory of dynamical system and show that a high dimensional system can be expressed, near critical transitions, in a very plain form but in an abstract (or latent) phase space. Thus, because of this particular feature, during this special phase, unlike during "business as usual" periods, we can detect the empirical signals of crisis approaching. The existence of such abstract system near critical transition points (e.g. a market distress) is guaranteed by the bifurcation theory and center manifold theory (see Arnold et al. (2013); Guckenheimer and Holmes (2013)). Hence, independently of the system complexity and the variables number, near transition phases we can describe the system in a simpler form. However, these variables are generally unobserved in the abstract phase space. Fortunately, if some of these unobserved factors first cross the transition point, a set of states and observable variables will display some particular statistical features (see Chen et al. (2012)). This group of variables represents the observable LTM in the original state space.

We shall establish that, when the system approaches a pre-crisis phase, the following generic temporal and spatial properties hold and that, if all these three conditions are satisfied simultaneously, the group of stocks fulfilling the requirements is called LTM. The three aforementioned statistical properties are:

- The presence of a group of stocks whose average Pearson's Correlation Coefficient (PCC) drastically increases in absolute value.
- The average PCC of stocks belonging to this group and any others stock in the system drastically decreases in absolute value.

- The average autocovariance (AC) of stocks in the group drastically increases in absolute value.

The drastic change in the properties of the LTM will reflect a transition to the crisis state.

The statistical characteristics of the LTM mimic some behavioral attitudes of market participants, as positive feedbacks and herding behaviors that reverberate in the path of stock prices. Indeed, the causes of various crashes in US and in other financial markets, e.g. in 1929, 1987, 2000 and 2008 could be traced back to herding behaviors and positive feedbacks in which the dynamics of aggregate variables depend on individual expectations and vice-versa (see e.g. Lux (1995, 1998); Anufriev et al. (2013); Hommes (2013)). On the one hand, in a financial environment where a self-organization process introduces positive feedbacks (see Zhou and Sornette (2003)) to the overall system, the future values of the stock price will depend on the present one, empirically translating into an increased autocovariance of stock returns; on the other hand, herding behavior effects (see Scheffer et al. (2009); Preis et al. (2011); Scheffer et al. (2012); Kefi et al. (2014); Moon and Lu (2015) among others), that lead agents to act collectively without a centralized direction, empirically drive an increase of the correlation (see Dakos et al. (2010)) of such returns. According to this view, financial crisis are specific features which stem from the non linear interactions among investor decisions (see Sornette (2017)).

The present approach is general and knuckles to a wider category of complex systems (e.g. ecosystems, climate systems, economic and financial system) characterized by sudden catastrophic shifts during the onset of a crisis phase (see e.g. Scheffer et al. (2001); Dakos et al. (2008); Quax et al. (2013)). A similar technique has been adopted in Chen et al. (2012) who proposed Dynamical Network Biomarkers (DNBs) to detect EWSs for the progression of complex diseases using throughput data. Differently from Chen et al. (2012), who look at the dispersion of the time series near a critical transition, in the detection of EWSs of financial crisis, beside variables co-movement, we are also keen in quantifying the self-similarity of the returns through the consideration of the autocovariance.

The three conditions discussed above represent a criterion for the proximity of a sudden change in a financial system, and their combination is naturally expected as a strong signal or an indicator for the pre-crisis state in financial markets. We thus define an aggregate indicator of financial crises based on the mean absolute value of the autocovariance of the financial instruments belonging to the LTMs and on the ratio between the correlations of stocks within the LTM and the correlations of stocks outside the leading module.

We apply this measure to predict abrupt transitions in financial markets such as systemic crises. In particular we aim at inferring major distress events on aggregate indices, representing the market as a whole, through the analysis of their constituents. In the construction of the early warning indicator, we disregard about the weight that each component has, to be as much agnostic as possible about how the constituents compound the aggregate system.

The rest of the paper is organized as follows: in Section 2 we revise the theoretical framework introduced by Chen et al. (2012), then we propose and describe our indicator for monitoring the proximity of a phase transition, demonstrating the utility of the empirical measures in signaling the proximity of a phase transition. In Section 3 we introduce an algorithm to extract the complex relationships from stocks' time series. The method is applied to empirical data, highlighting the goodness of the index via non parametric analysis of crisis episodes recognition, by comparing our technique to other well-accepted risk measures. Finally, Section 4 concludes.

2 The theoretical framework

The behavior of financial markets is very complicated and, in principle, it could be described by state equations in a high-dimensional space with several variables and parameters. Unfortunately this is an almost impossible task and some aggregation methods are necessary. It is in economics that the aggregation of variables has been mostly used as a technique to analyze the dynamics of high dimensional systems (see Simon and Ando (1961)). This behavior has lead to the practice of employing low dimensional systems to describe high dimensional environments (see e.g Barunik and Kukacka (2015); Diks et al. (2015); Diks and Wang (2016)).

Starting from this common approach, we employ dynamical system theory to demonstrate that a high dimensional system can be formulated in an abstract or latent phase space with a simpler form and that, by detecting some particular empirical signals, we can infer its critical transition. In other words, although the system's variables are generally unobserved, if some of them first cross the transition point, a set of state and observable variables will display some particular statistical features. This group of variables corresponds to the observable LTM in the original state space. In Section 2.1 we show the condition to detect the LTM in the original state space relating its statistical properties to the scheme of the unobserved variables in the abstract phase space.

2.1 A general model in abstract phase space

We describe the theoretical background that allows us to define the LTM following Chen et al. (2012), and derive a quantitative index as an EWS that announce the incoming of a transition phase.

Suppose the dynamics of a stock market can be described by the following dynamical system:

$$\mathbf{Z}(t+1) = f(\mathbf{Z}(t); P) + \varepsilon(t) \tag{1}$$

where $\mathbf{Z}(t) = (z_1(t), ..., z_n(t))$ is a n-dimensional state vector representing stocks, $P = (p_1, ..., p_s)$ is an s-dimensional parameter vector representing slowly changing factors (e.g. news on earnings or profits, anticipated takeovers or mergers, etc.) and $\varepsilon = (\varepsilon_1, ..., \varepsilon_n)$ is a n-dimensional stochastic component with ε_i Gaussian white noise with zero means and covariances κ_{ij}=$Cov(\varepsilon_i, \varepsilon_j)$. In general, $f : \mathbb{R}^n \times \mathbb{R}^s \to \mathbb{R}^n$ is a nonlinear vector-valued function. In order to apply theoretical results on bifurcations of a general discrete-time dynamical model, we consider only the deterministic skeleton of the system, i.e. we set $\varepsilon(t) = 0$. Furthermore, let us assume that the conditions below for Eq. (1) hold:

1. $\bar{\mathbf{Z}}$ is a fixed point of (1), that is $\bar{\mathbf{Z}} = f(\bar{\mathbf{Z}}; P)$;
2. there exists a value P_c such that one or a complex conjugate pair of the eigenvalues of the Jacobian matrix evaluated at the fixed point $\bar{\mathbf{Z}}$ is equal to 1 in modulus;
3. when $P \neq P_c$ the eigenvalues of the Jacobian matrix of (1) are generally not 1 in modulus.

These conditions, along with other transversality conditions, imply that the system undergoes a transition or a codimension-one bifurcation (see Chen et al. (2010)). The parameter P_c, at which the transition for the equilibrium value $\bar{\mathbf{Z}}$ occurs, is called a *bifurcation* value (or a critical transition value) where a sudden qualitative or topological change takes place. The bifurcation is generic from a mathematical viewpoint, i.e., almost all bifurcations for a general system satisfy these conditions.

Around the fixed point $\bar{\mathbf{Z}}$, it is possible to linearize the system described by Eq. (1) as:

$$\mathbf{Z}(t+1) \simeq \mathbf{J}(\mathbf{Z}(t) - \bar{Z}) \tag{2}$$

where $\mathbf{J} = \mathbf{J}(P)$ denotes the Jacobian matrix of (1). By defining $\mathbf{X} = \mathbf{Z} - \bar{\mathbf{Z}}$, it is possible to shift the fixed point to the origin, and the system characterized by Eq. (2) can be re-written as:

$$\mathbf{X}(t+1) = \mathbf{J}\mathbf{X}(t)$$

where $\mathbf{J}$ is a full rank matrix that also depends on the vector P.

Since the Jacobian matrix $\mathbf{J}$ is of full rank, then there exists a full-rank matrix $\mathbf{S}$ satisfying:

$$\mathbf{J} = \mathbf{S}\mathbf{\Lambda}\mathbf{S}^{-1}$$

By defining $\mathbf{Y} = \mathbf{S}^{-1}\mathbf{X}$, and reintroducing the stochastic component ε, the linearized version of the original system can be re-written as:

$$\mathbf{Y}(t+\Delta t) \simeq \mathbf{\Lambda}\mathbf{Y}(t) + \varepsilon(t) \tag{3}$$

By fixing the value of parameter P before reaching P_c, either $\mathbf{J}$ or $\mathbf{\Lambda}$ are constant matrices of full rank and we may end up with three cases: real and distinct eigenvalues, real and equal eigenvalues and complex eigenvalues.

If the sum of the dimensions of the eigenspaces with real eigenvalues is n, then there exists a non-singular matrix $\mathbf{S}$ satisfying $\mathbf{\Lambda} = \mathbf{S}^{-1}\mathbf{J}\mathbf{S} = diag(\lambda_1, ..., \lambda_n)$ being λ_i the i-th eigenvalue of the system (3). Without loss of generality, we may regard the first element $|\lambda_1|$ as being the nearest to 1, i.e., the dominant eigenvalue, whose change leads to the state shift from the fixed point. If matrix $\mathbf{J}$ does not have linearly independent eigenvectors, there exists a non-singular matrix $\mathbf{S}$ making $\mathbf{\Lambda}_2$ block diagonal. We can always move the block with the largest eigenvalue in modulus, which is also the nearest to 1, to the first position of $\mathbf{\Lambda}$. Finally, in the case of complex eigenvalues there exists a non-singular matrix $\mathbf{S}$ making $\mathbf{\Lambda}$ block diagonal where each two dimensional block matrix has a pair of complex conjugated eigenvalues whose moduli are less than 1. As before we move the block in which the eigenvalues have the largest modulus to the first position of $\mathbf{\Lambda}$. Therefore, irrespective of which case occurs, the first element of $\mathbf{\Lambda}$ is the dominant eigenvalue, i.e. the one nearest to 1 in modulus, whose change actually leads to the state shift from the fixed point. Furthermore, all the eigenvalues (or their moduli) of matrix $\mathbf{\Lambda}$ are within $[0, 1)$ and there is at least one dominant eigenvalue, approaching 1 in modulus when parameter $P \to P_c$.

For simplicity, we shall show the statistical properties of the original variables $\mathbf{Z}$ considering only the case of real and distinct eigenvalues, but the same conclusion applies for the other two cases in a similar manner (see Chen et al. (2012)).

Since $\mathbf{\Lambda}$ is a full diagonal matrix, as in Chen et al. (2012) we have that the variance $V(\cdot)$, the covariance $C(\cdot)$, the autocovariance $AC(\cdot)$ and the Pearson Correlation Coefficient $PCC(\cdot)$ of the autoregressive process expressed in Eq. (3) read as:

$$V\left(y_i(t)\right) = \frac{\kappa_{ii}}{1-\lambda_i^2} \tag{4}$$

$$C\left(y_i(t), y_j(t)\right) = \frac{\kappa_{ij}}{1-\lambda_i\lambda_j} \tag{5}$$

$$AC\left(y_i(t), y_i(t-1)\right) = \frac{\lambda_i\kappa_{ii}}{1-\lambda_i^2} \tag{6}$$

$$PCC\left(y_i(t), y_j(t)\right) = \frac{\kappa_{ij}}{\sqrt{\kappa_{ii}\kappa_{jj}}} \frac{\sqrt{\left(1-\lambda_i^2\right)\left(1-\lambda_j^2\right)}}{1-\lambda_i\lambda_j} \tag{7}$$

The dynamics of the original variables can be written as:

$$\begin{aligned} z_i\left(t\right) &= s_{i1}y_1\left(t\right) + ... + s_{in}y_n\left(t\right) + \bar{z}_i \\ z_j\left(t\right) &= s_{j1}y_1\left(t\right) + ... + s_{jn}y_n\left(t\right) + \bar{z}_j \end{aligned} \tag{8}$$

Thus, the variance and covariance of the original variables are given by:

$$V\left(z_i(t)\right) = s_{i1}^2 V\left(y_1(t)\right) + \sum\nolimits_{k=2}^{n} s_{ik}^2 V\left(y_k(t)\right) + \sum\nolimits_{k,m=1,k\neq m}^{n} s_{ik}s_{im}PCC\left(y_k(t), y_m(t)\right) \tag{9}$$

$$C\left(z_i(t), z_j(t)\right) = s_{i1}s_{j1}C\left(y_1(t)\right) + ... + s_{in}s_{jn}C\left(y_n(t)\right) + \sum\nolimits_{k,m=1,k\neq m}^{n} s_{ik}s_{im}PCC\left(y_k(t), y_m(t)\right) \tag{10}$$

The correlation is given by:

$$PCC\left(z_i(t), z_j(t)\right) = \frac{C\left(z_i(t), z_j(t)\right)}{\sqrt{V\left(z_i(t)\right)V\left(z_j(t)\right)}} \tag{11}$$

while the autocovariance reads as:

$$AC\left(z_i(t), z_i(t-1)\right) = s_{i1}^2 \lambda_1 V\left(y_1(t)\right) + \sum\nolimits_{k=2}^{n} s_{ik}^2 \lambda_k V\left(y_k(t)\right) + ...$$

$$... + \sum\nolimits_{k,m=1,k\neq m}^{n} s_{ik} s_{im} (\lambda_k + \lambda_m) PCC\left(y_k(t), y_m(t)\right) \tag{12}$$

Eqs. (11) and (12) relate the empirical signals of the original system (1) with the value assumed by the dominant eigenvalue of the latent system[1] in (3). The temporal and spatial statistical properties that signal a phase transition can thus be summarized as follows:

- If a variable z_i is related to y_1, that is, $s_{i1} \neq 0$, then the absolute value of the autocovariance $AC(z_i(t), z_i(t-1))$ increases greatly as $\lambda_1 \to 1$ otherwise it is bounded
- If variables z_i and z_j are related to y_1, that is, $s_{i1} \neq 0, s_{j1} \neq 0$ then $|PCC\left(z_i(t), z_j(t)\right)| \to 1$ as $\lambda_1 \to 1$
- If variables z_i and z_j are not related to y_1, that is $s_{i1} = 0, s_{j1} = 0$ then $|PCC\left(z_i(t), z_j(t)\right)| \to a$ with $a \in (0,1)$ as $\lambda_1 \to 1$
- If only variable z_i is related to y_1 but z_j is not, that is $s_{i1} \neq 0, s_{j1} = 0$ then $|PCC\left(z_i(t), z_j(t)\right)| \to 0$ as $\lambda_1 \to 1$

As in Chen et al. (2012), also in our case, each of the conditions represents a criterion to identify a phase transition, and their combination is naturally expected to be a stronger indicator for the pre-crisis state in financial markets.

We can thus develop an early warning indicator for determining the proximity of a financial crisis applying network concepts. Let $G_t = (N_t, E_t)$ represent a dynamical temporal graph with the set of nodes N_t put in correspondence with the variables $\mathbf{Z}_t$ of the original system denoting financial instruments (stocks) and a set of edges E_t representing the pairwise correlation $(PCC(z_i(t), z_t(t)))$ between each pair of instruments computed over a given moving window. The financial instruments can be divided in two groups: the subset of nodes $N_t^d \subset N_t$ belonging to the LTM, and the remaining subset $N_t^o = N_t \backslash N_t^d$ out of the leading module. If a networked

[1]It is worth to notice that an increase of the variance, covariance and autocorrelation of the original system could be due to both a proximity of a phase transition or a strong and unexpected exogenous shock in the stochastic component of the autoregressive process in (3).

system is approaching a transition point, the autocovariance of the financial instruments belonging to N_t^d increases; the correlation coefficients between stocks in N_t^d increase as well; finally, each correlation coefficient between a nodes in N_t^d and N_t^o reduces to 0.

Let $< |AC_t^d| >$ be the absolute mean value of the autocovariance of the nodes in N_t^d. Denote by $< |PCC_t^d| >$ the mean of the absolute value of the correlation coefficients between every pairs of nodes in N_t^d and $< |PCC_t^o| >$ the mean of the absolute value of the correlation coefficients between the nodes in N_t^d and the nodes in N_t^o. Then, our indicator for monitoring the proximity of a phase transition in financial markets can be defined as:

$$I_t^{AC} = \frac{< |AC_t^d| >< |PCC_t^d| >}{< |PCC_t^o| >} \tag{13}$$

Since our early warning indicator is dynamic by definition, it may be the case that a LTM is composed by a particular group of financial instruments that appears in a critical transition period but disappears in other periods, leaving the place to other stocks and signaling the upcoming of a new crisis. Therefore, the indicator I_t^{AC} always encompasses the stocks that potentially drive the system to a transition phase, but only when the indicator is sufficiently high, we are really in proximity of a transition.

In Appendix A we explore a Lotka-Volterra model of stock dynamics that serves as an example to demonstrate that the generated time series present the same statistical properties described above for the observable LTM. In other words, we propose a small-scale and conventional model to represent interdependencies among financial instruments by analyzing the dynamics of the variables near and far from phase transition confirming the theoretical results at the ground of our early warning indicator.

In the Appendix B we relate the dynamic of the LTM with the degree of decomposability of the Jacobian matrix of the unobserved system (see Simon and Ando (1961); Ando and Fisher (1963); Simon (1996); Courtois (2014)) showing how the degree of decomposability of $\mathbf{J}$ reduces as long as the dominant eigenvalue approaches the critical point.

3 Empirical analysis

The index presented in Eq. (13) results from the mixture of three different components, each of which has been proved to show a behavioral change near a critical transition. The index is expected to increase sharply (i.e. reaches maximum) when the financial system approaches a

critical transition that could eventually materialize in a systemic crisis. Therefore, I^{AC} may provide an early warning indicator to identify financial crises effectively.

To prove the efficacy of the indicator, we first describe the algorithm for finding the financial instruments belonging to the LTM, then the indicator is tested on the returns computed on the daily closure prices of three different stock markets (North America, Europe and Asia) during the period 2005-2018. The datasets are very heterogeneous and made up by different number of stocks from different geographical areas, and hit by different types of crises (e.g., the sub-prime financial crisis and the European Sovereign debt crisis).

3.1 The algorithm

Following Li et al. (2013), the steps of the algorithm for detecting the LTM at each time t can be summarized as:

- Log returns have been calculated from a $M \times T$ matrix containing the adjusted closure price time series of M stocks for T reporting days.
- A rolling window[2] of w working days has been applied at each time step t to extract the sub-matrix of the returns necessary for computing the value of the indicator at t. Thus, information embedded into I_t^{AC} regards only the stock market movements taking place in the time window[3] $[t-w;t]$.
- The resulting stocks are sorted in ascending order according to their autocovariance and only the highest x-percent of them are selected for the clustering procedure[4]. In this way, a group M_1 of stocks with a high AC_t at period t is obtained.
- The stocks are clustered based on the average correlation of their returns between periods $t-w$ and t. The optimal number of clusters has been found by maximizing the average Silhouette value[5].

[2] In Section 3.2 we have used various moving windows, ranging from one week to one month as a robustness check. We are aware about the existence of a trade-off between the statistically significance of a signal and its ability to timely intercept changes in the system's behaviors due to the moving window length. In the paper we have opted for a short moving window to endorse the forecasting power of the early warning indicator.

[3] It could happen that a stock has been dropped (or introduced) from the market in different periods. The algorithm uses only the stocks which have the complete series of prices from $t-w$ to t.

[4] In Section 3.2 we have let the threshold x vary from 100 to 40 percent as a robustness check.

[5] The Silhouette value is a measure of how similar a stock is to other stocks in its own cluster, when compared to stocks in other clusters. A high Silhouette value signals that a stock is well-matched to its own cluster, while it is poorly-matched to neighbor clusters.

- For each cluster H, we have computed the within absolute average correlation ($< |PCC_t^H| >$) and the between absolute average correlation ($< |PCC_t^{M_1 \setminus H}| >$) together with the absolute average autocovariance value $< |AC_t^H| >$ such that we have an index

$$I_t^{AC,H} = \frac{< |AC_t^H| >< |PCC_t^H| >}{< |PCC_t^{M_1 \setminus H}| >}$$

  for each cluster.

- The LTM at time t is the subset of stocks that has the maximum value of $I_t^{AC,H}$

$$I_t^{AC} = \max \left\{ I_t^{AC,H} \right\}$$

Algorithm 1: Early Warning Indicator I^{AC}

input : $M \times T$ matrix of stock prices P, a moving window w, a cut parameter x, the maximum number of clusters C

output: $1 \times T$ vector denoting the Early Warning Signal I^{AC}

$R \leftarrow \Delta(\log(P))$
$M \leftarrow \#stocks$
for $k \leftarrow 1$ **to** $T - w - 1$ **do**
  $r \leftarrow R(:, k : k + w)$
  $r_s \leftarrow r(sort(autocov(r))$
  $M_s \leftarrow M(sort(autocov(r))$
  $r_{ac} \leftarrow r_s(1 : x, :)$
  for $i \leftarrow 2$ **to** C **do**
    $r_{clust} \leftarrow cluster(r_{ac}, i)$
    $sil_i \leftarrow Silhouette(r_{clust})$
  $h \leftarrow max(sil_i)$
  $best_{clust} \leftarrow cluster(r_{ac}, h)$
  for $c \leftarrow 1$ **to** h **do**
    $H \leftarrow intersect(M_s, members(h(c))$
    $< |PCC^H| > \leftarrow mean(corr(r_{ac}(H)))$
    $< |AC^H| > \leftarrow mean(autocov(r_{ac}(H))$
    $< |PCC^{M_1 \setminus H}| > \leftarrow mean(corr(r_{ac}(M_1 \setminus H))$
    $I^{AC,H} \leftarrow \frac{<|AC^H|><|PCC^H|>}{<|PCC^{M_1 \setminus H}|>}$
  $t \leftarrow k + w$
  $I_t^{AC} \leftarrow max(I^{AC,H})$

The behavior of financial instruments belonging to the LTM characterizes the dynamic features of the corresponding financial system, since the members of the LTM make the first move from one state to another.

3.2 Application to stock markets

We apply the previously described methodology to three stock markets. For each dataset we consider the aggregate index and its constituents. The aggregate index dynamics is analyzed starting from the micro-level which is represented by the interactive behavior of its components. The first dataset we consider is the STOXX North America 600, a broad yet liquid subset of the STOXX Global 1800 Index with a fixed number of 600 components from US and Canada. The second dataset is the STOXX Europe 50 that gives a sketch of supersector leaders in Europe. It provides a basis for several investment products such as Exchange Traded Funds, Futures and Options, and structured products worldwide. The third dataset is the STOXX Asia/Pacific 600 with a fixed number of 600 components. All the data[6] have a daily frequency and range from 2005 to 2018. Finally, we remark that in the analysis we have employed the adjusted closure prices.

In order to test how our method proxies the effects of a distress, we employ standard approaches from crisis signaling (see Appendix C for the main technicalities on non-parametric analysis and forecasting accuracy evaluation). For an early warning model, two types of data are needed: vulnerability indicators and crisis events. The vulnerability indicators we use are the indicator I_t^{AC} developed in this paper, the method proposed by Chen et al. (2012) and an indicator resulting from the mix of both standard deviation and autocovariance, that is:

$$I_t^{AC,STD} = \frac{< |AC_t^d| >< |STD_t^d| >< |PCC_t^d| >}{< |PCC_t^o| >} \tag{14}$$

For crisis events we design two types of scenarios. In the first case, a crisis is a drop of at least 3% of the aggregate index returns and the leading indicator L we aim at mimicking takes value 1 from the dropping date to the whole previous month. In the second scenario a crisis is represented by a -4% in the returns of the aggregate index and a value of 1 is assigned to L at each day of the previous month but, differently from the previous case, the value 1 is assigned gradually day by day so that we can also evaluate the predictive power of the measures in anticipating a crisis event[7]. Additionally, we expound the results for the original signals and for

[6]The STOXX North America 600 represents the largest companies in the North America region. The STOXX Europe 50 covers stocks from Austria, Belgium, Czech Republic, Denmark, Finland, France, Germany, Ireland, Italy, Luxembourg, the Netherlands, Norway, Portugal, Spain, Sweden, Switzerland and the United Kingdom. The STOXX Asia/Pacific 600 represents basically the largest companies in Australia, Hong Kong, Japan, New Zealand and Singapore.

[7]In both cases the selected values represent extreme events that lie in the first percentile of the return distributions, as Figure 30 in Appendix H shows.

the smoothed ones, having applied the locally weighted regression fitting with a second order polynomial (LOESS).

An additional check involves the comparison of our measure with three well known indicators such as the Value at Risk (VaR) (see Jorion et al. (2007), Linsmeier and Pearson (2000)), the Marginal Expected Shortfall (MES) (see Oliviero et al. (2013)) and the Absorption Ratio (AR) (see Kritzman et al. (2010))[8]. The mathematical formulations of the three methods are reported in Appendix D.

The VaR gauges the maximum loss over a specific time horizon at a given confidence level. Besides, we do not assume that all past returns carry the same weight. Accordingly, we apply an exponential weighted moving average (EWMA) method to assign different weights, and in particular we consider exponentially decreasing weights (see Nieppola et al. (2009)). The MES evaluates the expected return on the portfolio in the worst $q\%$ of cases. The MES is an alternative to the VaR, being more sensitive to the shape of the tail of the loss distribution. Finally, the AR is defined as the fraction of covariation between asset returns induced by a prearranged number of eigenvectors. The AR grasps how much markets are unified or tightly coupled. In the latter case, markets become more fragile as negative shocks propagate faster and largely, compared to a situation in which markets are loosely linked. A large AR value corresponds to a high systemic risk level, being the sources of risk more unified.

In the main text we only report the results regarding the STOXX North America 600 dataset whereas we leave to the Appendices E.1-F the findings of the other two samples. The interpretation of the results and the main intuition apply to all the datasets while minor differences are described in Appendices E.1-F.

Since our early warning indicator is dynamic by definition, the group of stocks composing the LTM can change in time. In fact, the LTM can be formed by a certain set of financial instruments, near a particular critical transition phase, but such financial instruments can leave the place to other stocks inside the LTM, signaling the upcoming of a new crisis whose drivers are different from the ones leading to the previous turmoil. According to this view, how prices collapse is not the most important issue: a crash may occur because the market has entered an unstable phase and the subsequent turmoil may be fueled by any small disturbance. Figure 1 emphasizes how, near a crisis stage, the LTM appears from the cross correlation matrix (top left

[8]We are aware about the fact that newer and more refined measures of systemic risk exist nowadays; the choice of using the VaR, the MES, and the AR, on the other hand, is due to their wide dissemination as market standard risk measures.

Figure 1: **LTM and early warning indicators in different market phases.** The correlation matrix among stock returns together with the LTM is displayed for two different market phases, a distress (upper) and a business as usual (central) phase. From the plot it clearly emerges the increased correlation among LTM stocks during a financial crisis. Moreover the right panels show the percentage difference of the early warning indicators when computed on the LTM stocks or on the other modules. This difference increases during distress stages highlighting the importance of the LTM. The bottom panel reports the value of I^{AC}, I^{STD} and $I^{AC,STD}$ in 2008 and 2014. As expected the early warning indicators are higher in 2008.

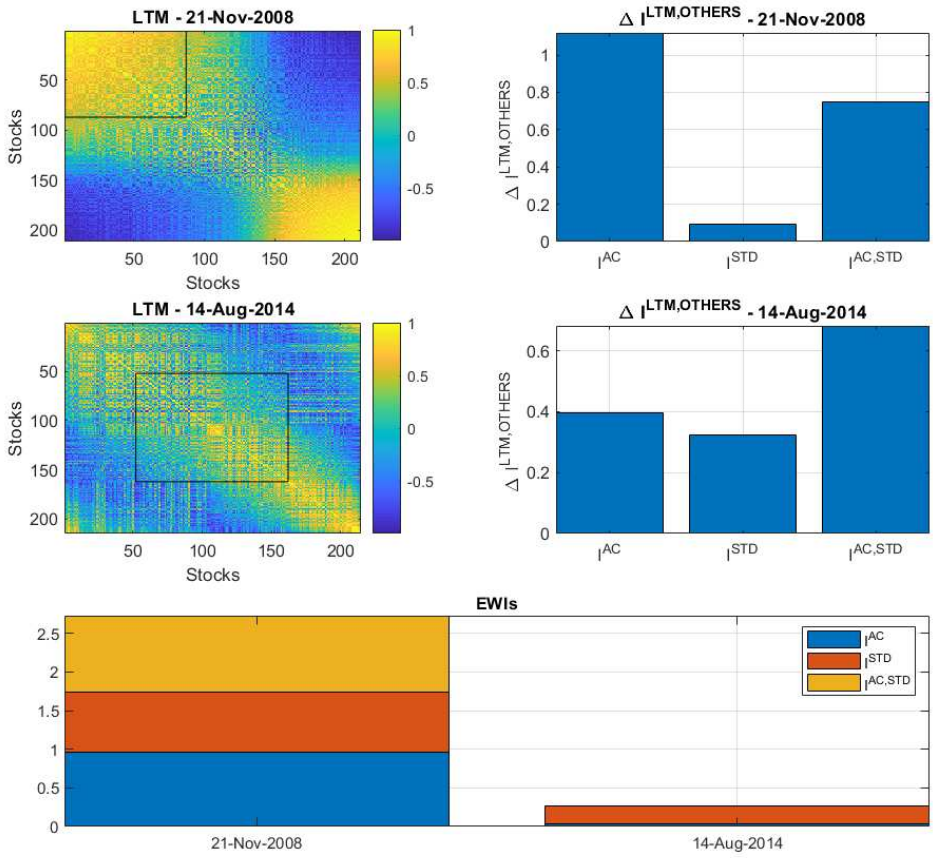

panel) while its occurrence is not strong during business as usual phases (central left panel). As a consequence, our early warning indicators, namely I^{AC} and $I^{AC,STD}$, assume higher values around the 2008 financial crisis if compared to a tranquil phase, as the top and central right panels display. More precisely, we have computed the difference between the indexes of the stocks belonging to the LTM and the ones belonging to the other modules. This comparison highlights the increasing magnitude of the proposed indicators when dealing with a period of financial distress. Finally, the bottom panels of Figure 1 report the cumulative sum of the three indicators I^{AC}, I^{STD} and $I^{AC,STD}$ in the two different dates and, as expected, we observe evident higher values in 2008.

Figure 2: **Early warning indicators patterns and the STOXX North America 600 aggregate index dynamic.** The three panels represent the original early warning indicators (red) together with the smoothed ones (black) and the STOXX North America 600 aggregate index (blue). The upper panel refers to the signal produced by using both autocovariance and standard deviation $I_t^{AC,STD}$ together with PCC. The central panel encompasses our proposed indicator which, beside PCC, relies only on autocovariance I_t^{AC}. The lower panel refers to the original indicator proposed by Chen et al. (2012) which is indicated with I_t^{STD}. In particular the label STD+AC refers to the mixed signal $I_t^{AC,STD}$, AC denotes our early warning indicator I_t^{AC} and finally STD refers to the I_t^{STD}.

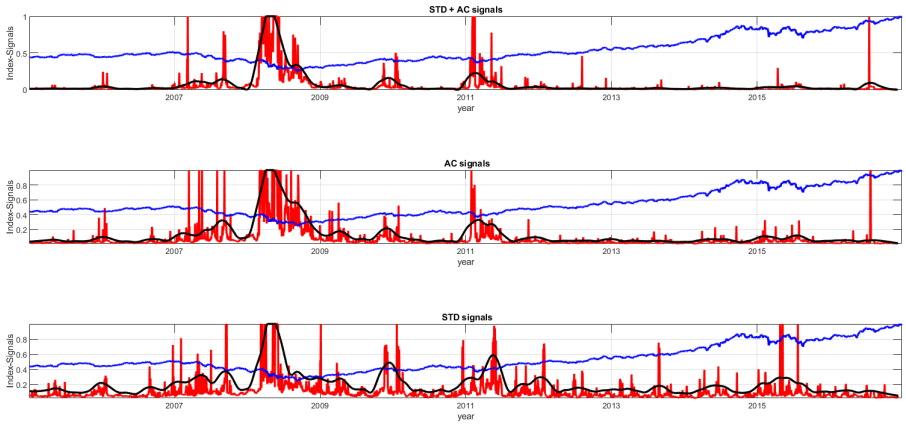

Figure 2 shows the signals produced by the three alternative methods. In particular the red lines refer to the original indicators while the black lines are the correspondent smoothed versions. We also plot, in blue, the STOXX North America 600 aggregate index to show how the indicators behave in different market phases. We have also normalized the index and the signals in a way that the maximum assumes value 1. This choice helps the comparison between the different signals. Besides the fact the signals behave similarly, the smoothed early warning indicators clearly indicate that our proposed technique, together with the mixed indicator, better discriminates between crisis and business as usual days. Indeed, both indicators assume low values in correspondence of tranquil phases while suddenly rise during crisis time. Instead the method proposed in Chen et al. (2012) generates a signal less able to distinguish between bad and good market times.

For a quantitative insight about the predictive power of the three methodologies, we report in Figure 3 the ROC and the PR curves obtained for the different signals. In the left panels we show the ROC curves while the right plots encompass the PR curves. The -4% crisis scenario in the top-left plot produces curves closer to the left-hand border and to the top border of the plotting space than those for the -3% (see the bottom-left subplot), thus indicating a more informative signal. Moreover we observe that our indicator overcomes the index proposed by

Figure 3: **ROC and PR curves for the two different crisis scenarios.** The left panels represent the ROC produced by the indicators while the right plots encompass the PR curves. The upper panels refer to the -4% crisis scenario while the bottom ones describe the results related to the -3% case. In each plot we report the original signals and the smoothed ones (SM). In particular the label STD refers to I_t^{STD}, AC denotes our early warning indicator I_t^{AC} and finally STD+AC refers to the mixed signal $I_t^{AC,STD}$.

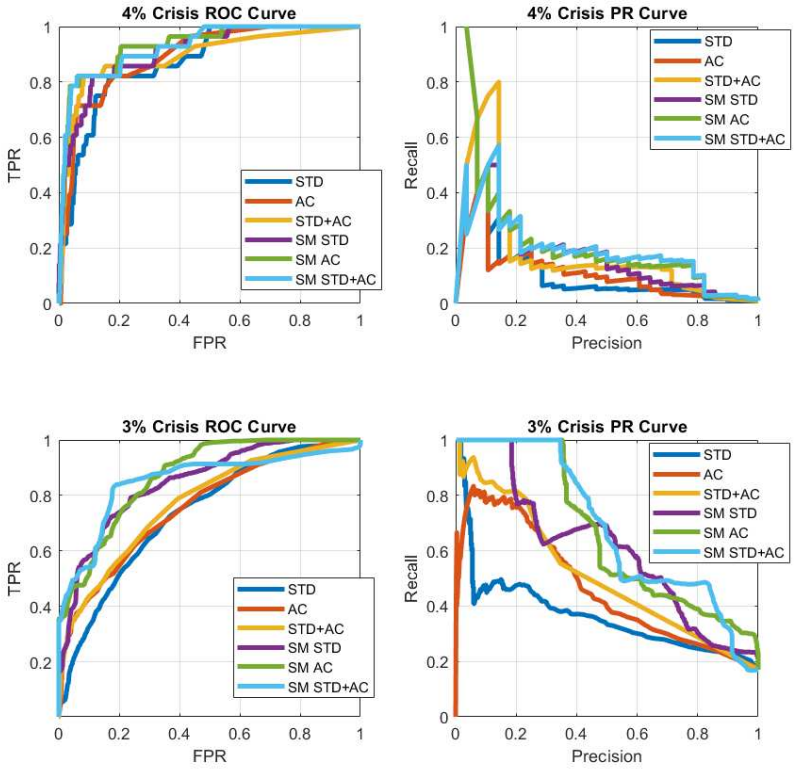

Chen et al. (2012), while the mixed early warning indicator provides only a slight increase in the performance. Generally speaking, we observe that smoothing the series has the effect of moving the curves upward since noises are washed out.

All the previous results refer only to a particular moving windows w used for computing the correlation between stock returns and, for the -4% crisis scenario also to a specific value of the leading indicator L. Figure 4 instead provides a broader view about the consistency of the results. We report the AUROC values for all the different moving windows w where we also consider varying time steps for the leading indicator L. As we expected, all methods provide better early warning signals near crisis periods, while the AUROC values decrease as long as we want to anticipate a market crash with a wider time horizon. Moreover this picture also provides evidence that our indicator together with the mixed signal outperforms the index of Chen et al. (2012).

Figure 4: **AUROC values for the two crisis scenarios and for different moving windows.** Each plot represents the AUROC obtained by varying the moving window w used to compute the correlation coefficients. The background colors refer to the AUROC values related to the -4% crisis scenario in which, beside the different windows, we also consider varying time steps for the leading indicator L. L takes value 1 gradually, day by day, up to one month behind the crisis event. The front line represents the AUROC for the -3% case where we consider the whole month for the leading indicator L. The upper panels represent the results related to the original early warning indicators while the bottom ones encompass results obtained for the smoothed signals. The different columns represent the results obtained for I_t^{STD}, I_t^{AC} and $I_t^{AC,STD}$ indicators respectively.

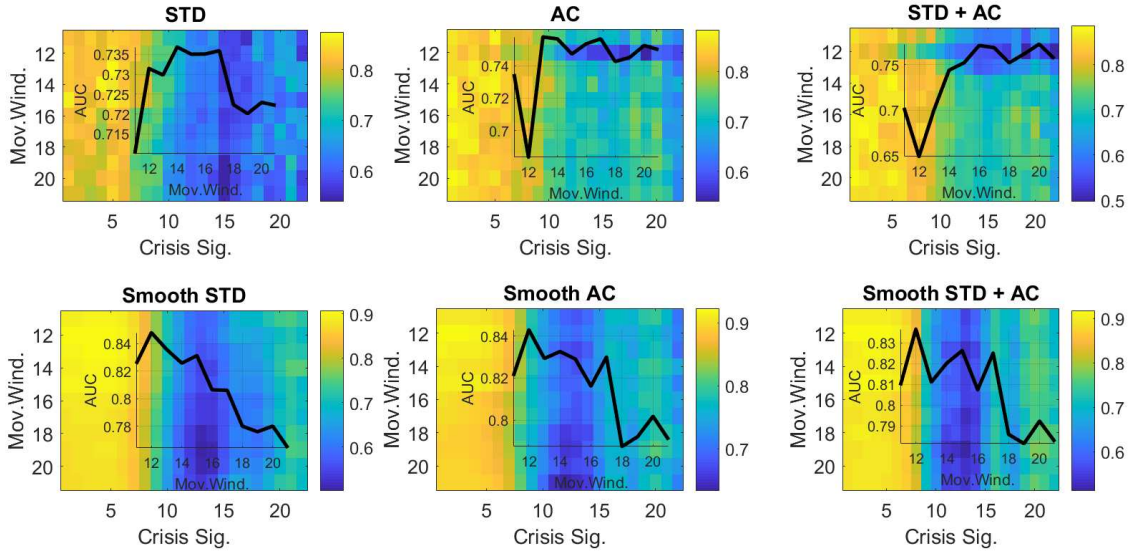

In particular, for the -4% crisis scenario, I_t^{STD} produces AUROC values in line with the other two signals (near 80%) up to one week, but then it shows a decreasing performance while both I_t^{AC} and $I_t^{AC,STD}$ tend to remain higher, approximately near 70%, up to a working month. Moreover, as previously observed, the smoothed signals increase the AUROC values around 90% near crisis events.

In order to check whether the previous outcomes are robust to changes in the value of the parameter x (representing the percentage of stocks selected for the clustering procedure) we show, in Figure 5, and report, in Table 1, the average AUROC values obtained by letting the parameter x vary from 100% to 40%. Each bar in Figure 5 represents the AUROC obtained by averaging the results of all the different moving windows (and of all the different values of the leading indicator L for the -4% crisis scenario) for a particular x.

From all the plots it clearly emerges that our proposed technique produces, on average, the highest AUROC values, outperforming the other two indices. The mixed signal comes second while I_t^{STD} follows. Notice that, in all the settings, our method generates quite high AUROC values, around 80%, meaning that it contains useful information to forecast crisis events. This

Figure 5: **Average AUROC for different settings of the parameter x defining the percentage of stocks with the highest autocovariance (or standard deviation) used for the clustering procedure.** Each plot represents the average AUROC obtained by varying the parameter x used to select the financial instruments with the highest autocovariance in the case of I_t^{AC} or standard deviation for, I_t^{STD}. These stocks are the ones used in the clustering procedure. The parameter x varies from 100% to 40%. For the mixed case we select the intersection of the stocks extracted by the previous settings. The upper panels refer to the -4% crisis scenario while the bottom ones describe the results for the -3% case. The left plots encompass results obtained by employing the originals signals while the two plots on the right refer to the smoothed cases.

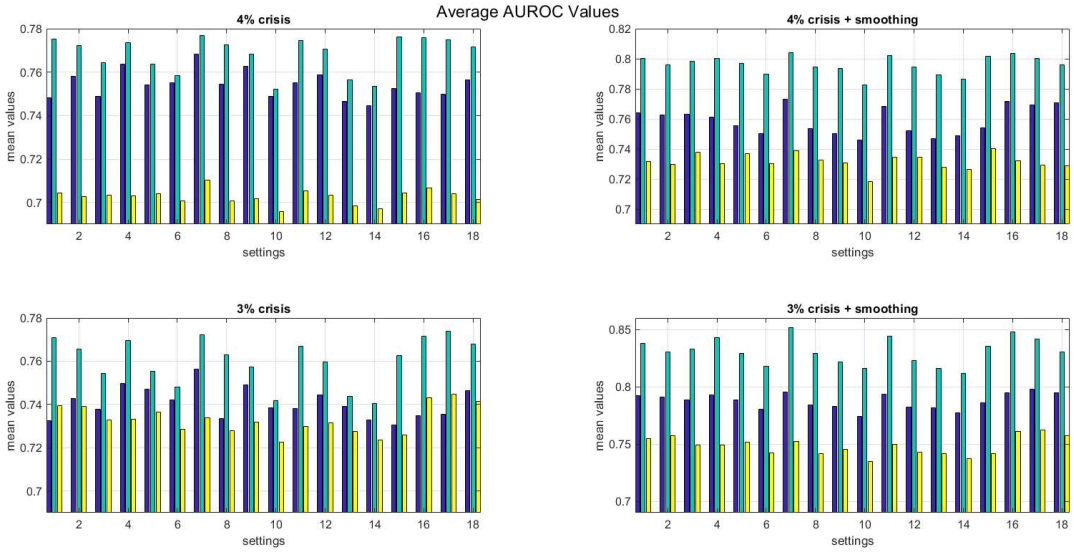

occurrence can be ascribed to the capability of the autocovariance in capturing the positive feedbacks generated on the market during pre-crisis phases. Only in the -3% crisis scenario the smoothed signals perform similarly. In Appendix G we also report the corresponding results associated with the average AUPR values.

Additionally, we have computed the series of the VaR, MES and AR adopting the identical moving window w used for I_t^{AC} and we have performed the same non-parametric analysis either in the -4% or in the -3% crisis scenarios. Afterwards, we have averaged the AUROC values obtained and compared them with the ones produced by our indicator. We have repeated this exercise for the raw VaR, MES and AR series as well as for the smoothed ones. Figure 6 reveals that our methodology always generates superior performances in signaling a crisis.

3.2.1 Policy evaluations

The literature on EWSs evaluation has been attempting to conceive a loss-function, able to determine the leak for a policymaker when considering a certain EWS, in a two-class setting (i.e. tranquil vs. crisis), in which the loss commonly derives from false alarms and missed

Table 1: **Average AUROC for different setting of the parameter x defining the percentage of stocks with the highest autocovariance (standard deviation) used for the clustering procedure.** The table represents the average AUROC obtained on changing the parameter employed to pick out the financial instruments featuring the highest autocovariance associated with I_t^{AC} or the largest standard deviation for I_t^{STD}. The parameter x varies from 100% to 40%. For the mixed case we select the intersection of the stocks extracted by the previous settings. The first three columns concern the -4% crisis scenario for $I_t^{AC,STD}$, I_t^{AC} and I_t^{STD} respectively. Columns from four to six regard the -4% crisis scenario and to the smoothed (SM) indicators. Columns from seven to nine refer to the -3% scenario while the last three columns collect the AUROC values of the smoothed (SM) indicators for the -3% crisis scenario.

4% Std + Ac	4% Ac	4% Std	4%-SM Std + Ac	4%-SM Ac	4%-SM Std	3% Std + Ac	3% Ac	3% Std	3%-SM Std + Ac	3%-SM Ac	3%-SM Std
0.7480	0.7752	0.7045	0.7642	0.8002	0.7317	0.7324	0.7709	0.7395	0.7921	0.8375	0.7546
0.7580	0.7723	0.7027	0.7628	0.7961	0.7296	0.7427	0.7656	0.7392	0.7912	0.8303	0.7569
0.7488	0.7642	0.7033	0.7629	0.7984	0.7376	0.7377	0.7544	0.7330	0.7882	0.8327	0.7493
0.7637	0.7737	0.7031	0.7610	0.8002	0.7303	0.7498	0.7694	0.7331	0.7926	0.8427	0.7493
0.7542	0.7638	0.7041	0.7556	0.7967	0.7367	0.7470	0.7554	0.7364	0.7886	0.8292	0.7519
0.7552	0.7583	0.7008	0.7502	0.7899	0.7304	0.7422	0.7480	0.7286	0.7805	0.8179	0.7425
0.7683	0.7770	0.7101	0.7732	0.8041	0.7389	0.7565	0.7721	0.7338	0.7953	0.8517	0.7524
0.7546	0.7725	0.7006	0.7538	0.7947	0.7326	0.7334	0.7631	0.7278	0.7842	0.8292	0.7413
0.7626	0.7682	0.7016	0.7504	0.7936	0.7306	0.7492	0.7572	0.7319	0.7827	0.8213	0.7456
0.7489	0.7523	0.6957	0.7459	0.7826	0.7185	0.7386	0.7417	0.7225	0.7742	0.8161	0.7345
0.7550	0.7745	0.7052	0.7684	0.8021	0.7347	0.7382	0.7670	0.7300	0.7932	0.8439	0.7494
0.7586	0.7706	0.7034	0.7520	0.7946	0.7346	0.7444	0.7597	0.7316	0.7824	0.8229	0.7431
0.7464	0.7565	0.6983	0.7471	0.7894	0.7277	0.7392	0.7438	0.7274	0.7813	0.8158	0.7415
0.7446	0.7535	0.6970	0.7487	0.7864	0.7262	0.7329	0.7406	0.7237	0.7769	0.8118	0.7373
0.7524	0.7760	0.7044	0.7538	0.8018	0.7403	0.7304	0.7626	0.7258	0.7857	0.8356	0.7414
0.7504	0.7758	0.7065	0.7717	0.8034	0.7319	0.7348	0.7715	0.7431	0.7946	0.8480	0.7608
0.7499	0.7748	0.7041	0.7693	0.8000	0.7294	0.7356	0.7739	0.7447	0.7976	0.8414	0.7621
0.7564	0.7715	0.7015	0.7705	0.7961	0.7289	0.7466	0.7678	0.7413	0.7946	0.8304	0.7571

Figure 6: **AUROC comparison.** The bars represent the average AUROC obtained by the VaR methodology, the MES and the AR along with the AUROC of our indicator I_t^{AC} for both the -4% and -3% crisis scenarios and for both the original signal and the smoothed (SM) one.

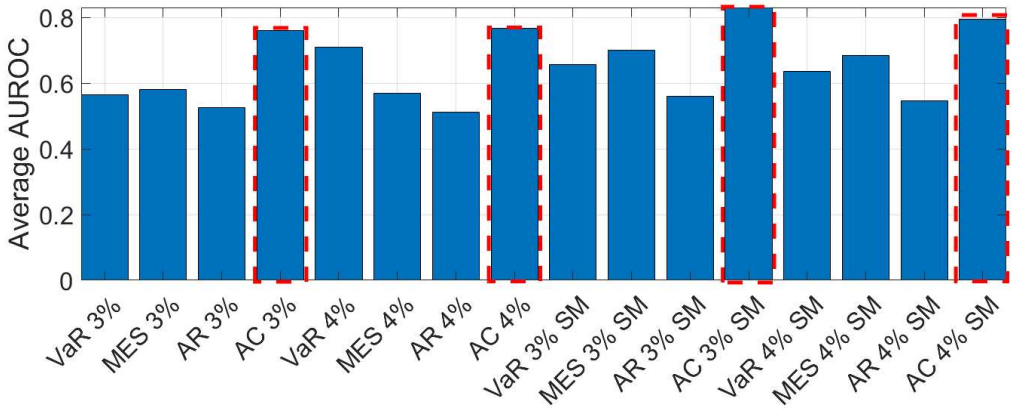

crises. To define the concepts of utility and relative utility as benchmark of classification performance (see Sarlin (2013)), we account for type I errors as the quota of missed crises with respect to the total crises frequency, i.e. $T_1 = FN/(FN + TP)$, while type II errors are the proportion of false alarms that are delivered with respect to the attendance of tranquil periods, i.e. $T_2 = FP/(TN + FP)$. Two further terms are also required: the policymakers' relative predilection μ between the two types of errors, which allows us to assess the potential unbalanced costs of errors, and the probabilities of crises P_1 and calm periods P_2 to esteem the

potential size difference between the two classes. Accordingly, a loss function is defined as:

$$Lo(\mu) = \mu T_1 P_1 + (1-\mu) T_2 P_2. \tag{15}$$

Further, based on this loss function, the absolute utility of the prediction model can be qualified through the comparison with what would be the best conjecture of a policymaker:

$$U_a(\mu) = \min(\mu P_1, (1-\mu) P_2) - L(\mu). \tag{16}$$

We also compute the relative usefulness, U_r, to contrast the absolute utility of the model to the absolute usefulness of a model with perfect performance ($Lo(\mu) = 0$). This exercise enables us to investigate whether and to what extent our signals I_t^{AC} is useful, which occurs when the loss obtained adopting of the model is smaller than the loss of disregarding it.

Table 2 provides the findings by applying the method developed in Sarlin (2013) to our early warning indicator. For an illustrative purpose, we report the outcomes for the -3% crisis scenario, averaged along different moving windows. In accordance with the literature, the evaluated performance indicates that the signal is beyond the best-guess of a policymaker and hence provides an overall positive usefulness. However, as expected (cf. Sarlin (2013)), the I_t^{AC} provides a higher utility only for policymakers more concerned with missing crises than issuing false alarms. Moreover we observe that, in general, the optimal thresholds decrease with increases in preferences μ, implying more signals with larger μ. This reflects the fact that, when the harm of a missing crises is larger, it is optimal to signal more.

Table 2: **Policy Analysis.** We report, for different measures of preference (μ), the absolute usefulness (Abs. Usef.), the relative usefulness (Rel. Usef.) and the optimal threshold (Thresh.) for different moving windows (MW), 10 days, 15 days and 20 days. Results refer to the -3% crisis scenario.

μ	Abs. Usef. MW-10d	Rel. Usef. MW-10d	Thresh. MW-10d	Abs. Usef. MW-15d	Rel. Usef. MW-15d	Thresh. MW-15d	Abs. Usef. MW-20d	Rel. Usef. MW-20d	Thresh. MW-20d
0.0000	-0.0000	NaN	0.4159	0.0000	NaN	0.4626	0.0000	NaN	0.3893
0.1000	0.0002	0.0100	0.3570	0.0004	0.0214	0.3162	0.0002	0.0138	0.3893
0.2000	0.0018	0.0523	0.0728	0.0017	0.0505	0.1314	0.0008	0.0231	0.2357
0.3000	0.0054	0.1049	0.0558	0.0047	0.0924	0.0828	0.0039	0.0760	0.0527
0.4000	0.0096	0.1411	0.0507	0.0093	0.1358	0.0697	0.0086	0.1257	0.0423
0.5000	0.0146	0.1714	0.0406	0.0148	0.1739	0.0607	0.0146	0.1710	0.0350
0.6000	0.0209	0.2044	0.0311	0.0213	0.2087	0.0528	0.0223	0.2173	0.0287
0.7000	0.0300	0.2522	0.0222	0.0299	0.2508	0.0349	0.0316	0.2648	0.0227
0.8000	0.0443	0.3257	0.0109	0.0440	0.3231	0.0148	0.0444	0.3252	0.0096
0.9000	0.0165	0.1984	0.0043	0.0178	0.2144	0.0051	0.0158	0.1907	0.0037
1.0000	0.0000	NaN	0.0010	0.0000	NaN	0.0010	0.0000	NaN	0.0010

Moreover, with the aim of providing an exploitable tool to policymakers, our indicator is discretized to obtain thresholds indicating a tranquil or a crisis period. To overcome the problem on having a continuous variable difficult to interpret, a Hidden Markov Model (HMM) is proposed on top of the indicator previously described for signaling a possible distress period.

A HMM hypothesizes that an observation at a certain time t is engender by some process, whose state S_t is not observable. Moreover, the nature of the underlying process satisfies the Markov properties. Both properties imply that the joint distribution of a string of states and observations can be factorized as:

$$P(S_{1:T}, Y_{1:T}) = P(S_1)P(Y_1|S_1)\prod_{t=2}^{T} P(S_t|S_{t-1})P(S_t|Y_t) \tag{17}$$

To define a probability distribution over sequences of observations, we need to specify a probability distribution $P(S_1)$ over the initial state, the state transition matrix $K \times K$ defining $P(S_t|S_{t-1})$ and the output model $P(Y_t|S_t)$. HMMs usually assume that the state transition matrices and the output models are time invariant (except for the initial state). If the observable variables are discrete, the output can be entirely precised by a $K \times L$ emission matrix. We remark that, for the transition matrices estimation from the observed sequence of emissions, we adopt the Baum-Welch algorithm (see Durbin et al. (1998); Eddy (1998)).

For each time period we have multiplied the signal I_t^{AC} for 10000 to get results in basis points; these values are then rounded to the closest integer number. This measure can be seen as the time emanation of the HMM. Then we have assumed that such emissions are caused by an underlying synchronization categorical variable, with Em unobserved states. We let Em be equal to three hidden levels, portraying them as signaling low, medium and high levels of financial distress. From an econometric perspective, hidden levels represent regime switching states. Using a HMM, at each time point, the most likely level of distress, among the three possible states, are achievable. Figure 7 shows the course of the estimated levels.

The HMM estimated states show an enhancement in the level of distress, starting in the second half of 2007 and that came to a peak in the summer of 2009. The financial crisis moved the level of distress from an initial low degree, then to a medium and finally to a huge level in 2009. However, it reverted to a medium state in the subsequent few years, until the 2011 European Sovereign debt crisis took place. Moreover, at the end of the sample it seems that the system stabilizes at a low level of distress, apart from isolated events as the turmoil after the devaluation of the Chinese Renmimbi in the summer of 2015.

Figure 7: **Discretization of the signal I_t^{AC} obtained through a Hidden Markov Model.** The figure presents the three states obtained by the discretization of the original signal I_t^{AC}. The blue bars, ranging from the lightest to the darkest, represent the low (cyan), medium (light blue) and high (dark blue) level of the system's distress while the red line denotes the STOXX North America 600 aggregate index.

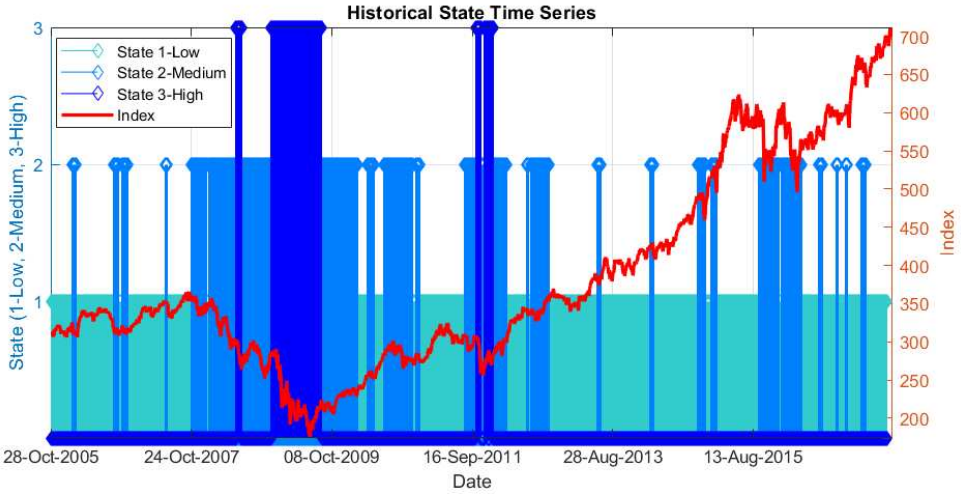

4 Conclusions

The present work has considered a novel model-free method for detecting EWSs of financial crises starting from a complex system perspective applied to financial markets, according to which crisis represent innermost properties of the system. By analyzing the demeanor of a group of stocks, the Leading Temporal Module, we have proposed an aggregated early warning indicator to predict financial downturns. The method is general and counts on the occurrence of some peculiar statistical features displayed by the LTM at the crossing of the transition point. These characteristics are: an increase in the autocovariance, a boost in the correlation between the members of the LTM and a decrease of the correlation between the stocks in that group and the rest of the financial instruments.

To test the usefulness and the broad validity of the approach we have exploited data covering various geographical area and crisis episodes. We have considered North America, Europe, and Asia-Pacific stock market indices for the period 2005-2018 such that either major global financial crisis events or different local triggers have been mapped.

We have investigated the aggregate indices' dynamics by starting from the micro-level embodied by the interactive behavior of their components. By adopting a non-parametric approach, we have shown either the capability of our indicator to detect systemic crisis or its superiority in terms of forecasting performances with respect to well accepted measures of systemic risk. This supports the goodness of our early warning indicator for macro-prudential monitoring and risk

assessment.

The broad generality of the proposed approach opens room for its applicability to different environments, e.g. other financial markets, OTC markets, real micro-series like consumption and investment streams. More interestingly, this methodology could be potentially applied to real-time data sets to identify and timely forecast major breakdowns, and thus helping policy-makers in making more informed policy decisions.

References

Ando, A. and Fisher, F. M. (1963). Near-decomposability, partition and aggregation, and the relevance of stability discussions. *International Economic Review*, 4(1):53–67.

Anufriev, M., Hommes, C. H., and Philipse, R. H. (2013). Evolutionary selection of expectations in positive and negative feedback markets. *Journal of Evolutionary Economics*, 23(3):663–688.

Arnold, V. I., Afrajmovich, V., Il'yashenko, Y. S., and Shil'nikov, L. (2013). *Dynamical systems V: bifurcation theory and catastrophe theory*, volume 5. Springer Science & Business Media.

Barunik, J. and Kukacka, J. (2015). Realizing stock market crashes: stochastic cusp catastrophe model of returns under time-varying volatility. *Quantitative Finance*, 15(6):959–973.

Bisias, D., Flood, M., Lo, A. W., and Valavanis, S. (2012). A survey of systemic risk analytics. *Annu. Rev. Financ. Econ.*, 4(1):255–296.

Chen, L., Liu, R., Liu, Z.-P., Li, M., and Aihara, K. (2012). Detecting early-warning signals for sudden deterioration of complex diseases by dynamical network biomarkers. *Scientific reports*, 2:342.

Chen, L., Wang, R., Li, C., and Aihara, K. (2010). *Modeling biomolecular networks in cells: structures and dynamics*. Springer Science & Business Media.

Courtois, P. J. (2014). *Decomposability: queueing and computer system applications*. Academic Press.

Dakos, V., Carpenter, S. R., Brock, W. A., Ellison, A. M., Guttal, V., Ives, A. R., Kefi, S., Livina, V., Seekell, D. A., Van Nes, E. H., et al. (2012). Methods for detecting early warnings of critical transitions in time series illustrated using simulated ecological data. *PloS one*, 7(7):e41010.

Dakos, V., Scheffer, M., Van Nes, E. H., Brovkin, V., Petoukhov, V., and Held, H. (2008). Slowing down as an early warning signal for abrupt climate change. *Proceedings of the National Academy of Sciences*, 105(38):14308–14312.

Dakos, V., Van Nes, E. H., Donangelo, R., Fort, H., and Scheffer, M. (2010). Spatial correlation as leading indicator of catastrophic shifts. *Theoretical Ecology*, 3(3):163–174.

Davis, E. P. and Karim, D. (2008). Comparing early warning systems for banking crises. *Journal of Financial stability*, 4(2):89–120.

Diks, C., Hommes, C., and Wang, J. (2015). Critical slowing down as early warning signals for financial crises. Technical report.

Diks, C. and Wang, J. (2016). Can a stochastic cusp catastrophe model explain housing market crashes? *Journal of Economic Dynamics and Control*, 69:68–88.

Durbin, R., Eddy, S. R., Krogh, A., and Mitchison, G. (1998). *Biological sequence analysis: probabilistic models of proteins and nucleic acids*. Cambridge university press.

Eddy, S. R. (1998). Profile hidden markov models. *Bioinformatics (Oxford, England)*, 14(9):755–763.

Farmer, J. D. (2000). A simple model for the nonequilibrium dynamics and evolution of a financial market. *International Journal of Theoretical and Applied Finance*, 3(03):425–441.

Fisher, F. M. and Ando, A. (1962). Two theorems on ceteris paribus in the analysis of dynamic systems. *American Political Science Review*, 56(1):108–113.

FSB (2011). Macroprudential policy tools and frameworks. progress report to the g-20. Technical report, Financial Stability Board.

Guckenheimer, J. and Holmes, P. (2013). *Nonlinear oscillations, dynamical systems, and bifurcations of vector fields*, volume 42. Springer Science & Business Media.

Haldane, A. G. and May, R. M. (2011). Systemic risk in banking ecosystems. *Nature*, 469(7330):351.

Hommes, C. (2013). *Behavioral rationality and heterogeneous expectations in complex economic systems*. Cambridge University Press.

IMF (2011). Macroprudential policy: An organizing framework. Technical report, International Monetary Fund.

Jorion, P. et al. (2007). *Financial risk manager handbook*, volume 406. John Wiley & Sons.

Kefi, S., Guttal, V., Brock, W. A., Carpenter, S. R., Ellison, A. M., Livina, V. N., Seekell, D. A., Scheffer, M., Van Nes, E. H., and Dakos, V. (2014). Early warning signals of ecological transitions: methods for spatial patterns. *PloS one*, 9(3):e92097.

Kritzman, M., Li, Y., Page, S., and Rigobon, R. (2010). Principal components as a measure of systemic risk.

Lee, S.-J., Lee, D.-J., and Oh, H.-S. (2005). Technological forecasting at the korean stock market: A dynamic competition analysis using lotka–volterra model. *Technological Forecasting and Social Change*, 72(8):1044–1057.

Li, M., Zeng, T., Liu, R., and Chen, L. (2013). Detecting tissue-specific early warning signals for complex diseases based on dynamical network biomarkers: study of type 2 diabetes by cross-tissue analysis. *Briefings in bioinformatics*, 15(2):229–243.

Linsmeier, T. J. and Pearson, N. D. (2000). Value at risk. *Financial Analysts Journal*, 56(2):47–67.

Lorenzoni, G. and Werning, I. (2013). Slow moving debt crises. Technical report, National Bureau of Economic Research.

Lux, T. (1995). Herd behaviour, bubbles and crashes. *The economic journal*, pages 881–896.

Lux, T. (1998). The socio-economic dynamics of speculative markets: interacting agents, chaos, and the fat tails of return distributions. *Journal of Economic Behavior & Organization*, 33(2):143–165.

May, R. M., Levin, S. A., and Sugihara, G. (2008). Complex systems: Ecology for bankers. *Nature*, 451(7181):893.

Moon, H. and Lu, T.-C. (2015). Network catastrophe: self-organized patterns reveal both the instability and the structure of complex networks. *Scientific reports*, 5:9450.

Nieppola, O. et al. (2009). Backtesting value-at-risk models.

Oliviero, R., Edward, A., et al. (2013). *Managing And Measuring Of Risk: Emerging Global Standards And Regulations After The Financial Crisis*, volume 5. World Scientific.

Preis, T., Schneider, J. J., and Stanley, H. E. (2011). Switching processes in financial markets. *Proceedings of the National Academy of Sciences*, 108(19):7674–7678.

Quax, R., Kandhai, D., and Sloot, P. M. (2013). Information dissipation as an early-warning signal for the lehman brothers collapse in financial time series. *Scientific reports*, 3:1898.

Rhu, H.-K. et al. (2011). Macroprudential policy framework. *BIS Papers chapters*, 60:120–123.

Samuelson, P. A. (1971). Generalized predator-prey oscillations in ecological and economic equilibrium. *Proceedings of the National Academy of Sciences*, 68(5):980–983.

Sarlin, P. (2013). On policymakers loss functions and the evaluation of early warning systems. *Economics Letters*, 119(1):1–7.

Scheffer, M., Bascompte, J., Brock, W. A., Brovkin, V., Carpenter, S. R., Dakos, V., Held, H., Van Nes, E. H., Rietkerk, M., and Sugihara, G. (2009). Early-warning signals for critical transitions. *Nature*, 461(7260):53.

Scheffer, M., Carpenter, S., Foley, J. A., Folke, C., and Walker, B. (2001). Catastrophic shifts in ecosystems. *Nature*, 413(6856):591.

Scheffer, M., Carpenter, S. R., Lenton, T. M., Bascompte, J., Brock, W., Dakos, V., Van de Koppel, J., Van de Leemput, I. A., Levin, S. A., Van Nes, E. H., et al. (2012). Anticipating critical transitions. *Science*, 338(6105):344–348.

Simon, H. A. (1996). *The architecture of complexity*. Cambridge, MA: MIT Press.

Simon, H. A. and Ando, A. (1961). Aggregation of variables in dynamic systems. *Econometrica*, 29(2):111–138.

Solomon, S. and Richmond, P. (2001). Power laws of wealth, market order volumes and market returns. *Physica A: Statistical Mechanics and its Applications*, 299(1-2):188–197.

Sornette, D. (2003). Critical market crashes. *Physics Reports*, 378(1):1–98.

Sornette, D. (2017). *Why stock markets crash: critical events in complex financial systems*. Princeton University Press.

Thompson, G. (2011). Sources of financial sociability: networks, ecological systems or diligent risk preparedness? *Journal of Cultural Economy*, 4(4):405–421.

Wilkinson, J. H. (1965). *The algebraic eigenvalue problem*, volume 87. Clarendon Press Oxford.

Zhou, W.-X. and Sornette, D. (2003). 2000–2003 real estate bubble in the uk but not in the usa. *Physica A: Statistical Mechanics and its Applications*, 329(1-2):249–263.

A A stylized model of stock interactions

The stock market can be perceived as an ecosystem where traders compete for resources, that is the values of the companies being traded, or as a collection of stocks competing for the investors' wealth. Traders drop in and out of the market and may occasionally switch between their trading strategies; additionally stocks may disappear from market indices and new stocks can replace them. The mathematical relationships which describe the connections between companies or stocks can be compared to those describing the extinction (or survival) mechanism of biological species in natural ecosystems, as in a Lotka-Volterra model. Indeed, Thompson (2011) considers *the financial system as akin to an ecological network* while May et al. (2008) and Haldane and May (2011) draw analogies between the dynamic of ecological systems and financial networks. The latter adopts the notion of financial ecosystem, in which evolutionary forces have often been survival of the biggest rather than the fittest. We recall that several contributions adopt the same Lotka-Volterra framework to investigate financial markets dynamics (see e.g. Samuelson (1971); Farmer (2000); Solomon and Richmond (2001); Lee et al. (2005)).

The equations that constitute the model are:

$$z_i(t+1) = b_i z_i(t) + \sum_{j=1}^{4} Q_{ij} z_j(t) z_i(t) + \epsilon_i \tag{18}$$

where the stock[9] prices are denoted by z_i and b_i represents the maximum rate of change of each stock which is also subject to a noise term ϵ_i, referring to short-term fluctuations in the rate of change of the stock price.

The interactions between stocks are encompassed in the matrix Q, for which we consider the following specification:

$$Q = \begin{pmatrix} -.1 & .02 & -.1 & -.1 \\ .02 & -.1 & -.1 & -.1 \\ -.1 & -.1 & -.1 & .02 \\ -.1 & -.1 & .02 & -.1 \end{pmatrix}$$

Each entry describes the strength and the direction of the interaction between stocks. In particular, negative coefficients signal stocks suppressing each other while positive terms refer to enhancement. Economically, we can interpret negative interactions as being originated by the

[9] We adopted a model with only 4 stocks as a minimal model to design stocks interactions. The results also apply to a larger set of stocks.

substitutability of stocks and positive interactions as the results of the complementarity between pairs of financial instruments.

The simulations of the model are useful to identify sharp transitions from a dynamical regime to another, as it is often observed in complex systems, such as ecosystems, engineering networks, social organizations and financial markets (see Sornette (2003); Davis and Karim (2008); Scheffer et al. (2012); Dakos et al. (2012)). Such *regime shifts* are frequently arising from external shocks. However, it might be the case that a slight perturbation can lead to a substantial transition to a new and permanent state (see Lorenzoni and Werning (2013)).

In the analysis, we let b_3 and b_4 vary from 0.5 to 1.5 and show how the statistical properties of the simulated time series change as long as these parameters assume different values. Specifically, while far from transition, time series exhibit relatively low autocovariance and also low correlation, near the transition point the fluctuations exhibit higher volatility and autocovariance and the correlation between the stocks also becomes stronger. Concurrently, we evaluate how the dominant eigenvalue varies while approaching the transition point. Figure 8 shows, in red, the values of the average autocovariance (top panel) and the average correlation (top bottom panel), while in blue we depict the absolute values of dominant eigenvalue. Notice that $|\lambda_1|$ reaches 1 when b_3 and b_4 approach 0.95. Near this value both the autocovariance and the average correlation approach their maximum value highlighting the transition.

Figure 8: **Empirical signals and leading eigenvalue dynamics for different bifurcation parameters.** The model simulations illustrate generic indicators of phase transition (red lines) along with the absolute value of the dominant eigenvalue (blue). The average autocovariance is reported in the top panel while the average correlation values are shown in bottom panel.

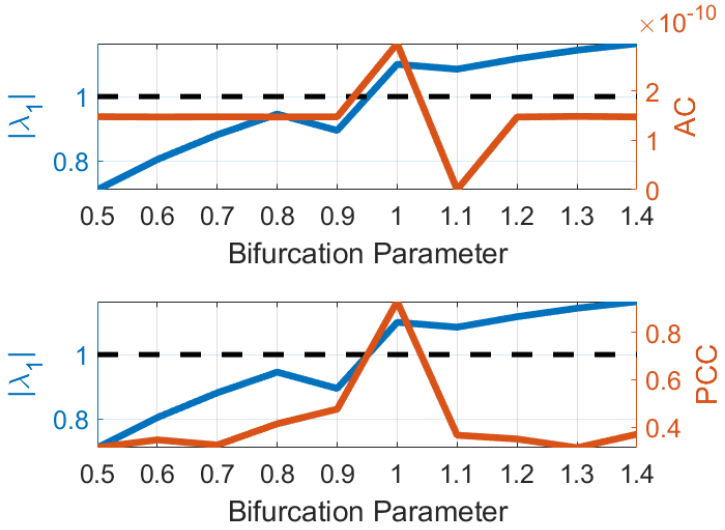

B Leading temporal module and matrix decomposability

The appearance of a set of variables that drives the system to a transition phase can be linked to the degree of decomposability[10] of the Jacobian matrix (see Simon and Ando (1961); Ando and Fisher (1963); Simon (1996); Courtois (2014)) of the unobserved underlying system. The modification in the properties of this group is indeed the empirical reflection of a reduced level of decomposability of the matrix. The decomposability (see Simon and Ando (1961); Ando and Fisher (1963); Simon (1996); Fisher and Ando (1962)) of the Jacobian matrix $\mathbf{J}$ in Eq. (3) is intimately connected to the emergence of a transition phase and, accordingly, related to the empirical signals that lead to the arising of the LTM. In what follows, how the decomposability degree of $\mathbf{J}$ reduces as long as the dominant eigenvalue approaches the critical point is shown. To do so, the eigenvectors $\mathbf{S}(P_c)$ of the Jacobian matrix $\mathbf{J}(P_c)$ at the critical point P_c are approximated as functions of the eigenvectors $\mathbf{S}$ of $\mathbf{J}$ far from the transition state. Following Wilkinson (1965), we use the eigenvectors $\mathbf{S}$ of $\mathbf{J}$ as a base to express the set of eigenvectors $\mathbf{S}(P_c)$ of $\mathbf{J}(P_c)$.

As in Courtois (2014), we have that:

$$s_{i,k}(P_c) = \sum_x \beta_{x,k} s_{i,x} \tag{19}$$

where β is the eigenvectors matrix of $\mathbf{S}^{-1}\mathbf{J}(P_c)\mathbf{S}$. In particular, the dominant eigenvector $\mathbf{S}_1(P_c)$ can be written as:

$$s_{i,1}(P_c) = \beta_{1,1} s_{i,1} + \sum_{x=2} \beta_{x,1} s_{i,x} \tag{20}$$

Courtois (2014) proved that the modulus of $\beta_{k,1}$, $k \neq 1$, expresses the degree of indecomposability of $\mathbf{J}$ and that it decreases as the degree of indecomposability increases. Thus, from Equation (21) it follows that:

$$\frac{s_{i,1}(P_c)}{s_{i,1}} = \beta_{1,1} + \frac{\sum_{x=2} \beta_{x,1} s_{i,x}}{s_{i,1}} \tag{21}$$

meaning that the empirical signals produced by the observable variables are the immediate reflection of the manifestation of a critical transition of the system in the abstract phase space, i.e. $|s_{i,1}(P_c)| > |s_{i,1}|$ which holds if $\left|\beta_{1,1} + \frac{\sum_{x=2} \beta_{x,1} s_{i,x}}{s_{i,1}}\right| > 1$.

Employing the Lotka-Volterra model for stock interactions presented in Section A, we demon-

[10] A decomposable matrix is a square matrix such that a rearrangement of its rows and columns generates a set of square submatrices on the principal diagonal and zeros elsewhere.

strate how the values of $\beta_{x,k}$ are related to the phase transition of the system. Figures 9 shows the decomposability degree $\sum_{x=2}\beta_{x,1}$ on the upper panel while $\beta_{1,1}$ is reported in the bottom panel. The blue line represents the absolute value of the dominant eigenvalue and it reaches 1 when b_3 and b_4 approach 0.95. Near the transition value, the decomposability of the Jacobian matrix reduces, i.e. the number of square submatrices on the principal diagonal increases, and the first entry of $\beta_{x,1}$ peaks signaling a stronger relationships between the empirical signals and the theoretical model. To analyze the conduct of the early warning indicator I^{AC} as long

Figure 9: **Decomposability signals and dominant eigenvalue dynamics for different parameter values.** The simulations illustrate the generic decomposability indicators (red lines) along with the absolute value of the leading eigenvalue (blue). The values of $\sum_{x=2}\beta_{x,1}$ are reported in the top panel while the values of $\beta_{1,1}$ are shown in the bottom panel.

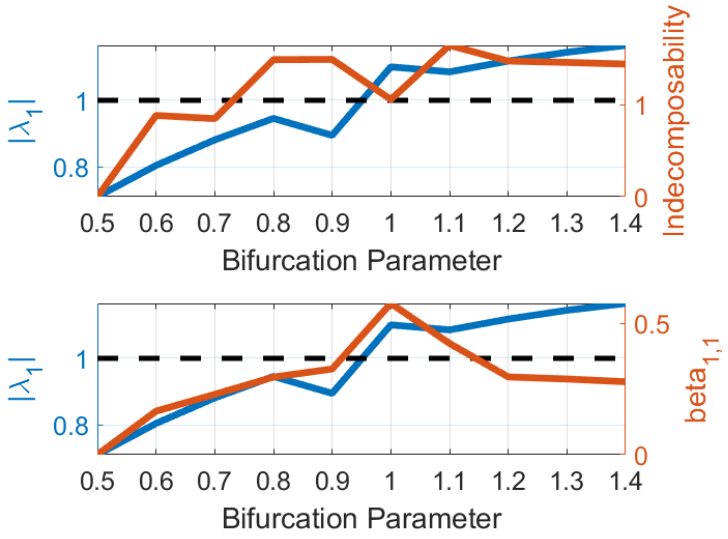

as $\mathbf{S}$ and $\mathbf{\Lambda}_2$ vary, we generate synthetic data from the following data generating process that reproduces the model of Section 2:

$$\mathbf{Z}(t) = \mathbf{S}\mathbf{Y}(t)$$

$$\mathbf{Y}(t+1) = \mathbf{\Lambda}\mathbf{Y}(t) + \varepsilon(t)$$

We have created different configurations of $\mathbf{S}$ and $\mathbf{\Lambda}_2$ by changing the features of the Jacobian matrix $\mathbf{J}$ and then by computing its eigenvalues $\mathbf{\Lambda}$ and eigenvectors $\mathbf{S}$. The Jacobian takes the following form:

$$\mathbf{J} = \mathbf{J}^* + \delta\hat{\mathbf{J}}$$

where $\mathbf{J}^*$ is diagonal and $\hat{\mathbf{J}}$ encompasses the values outside the main diagonal. In this way, tuning the parameter δ we can let the degree of decomposability of $\mathbf{J}$ to assume different levels.

We study how the algorithm reacts to these changes. For this purpose, we have produced two series of synthetic datasets considering $n = 20$ stocks, whose price pattern has been simulated for $t = 100$ periods. The variance of ε has been set to 0.5 but, in the first series we have assumed $\delta = 0.01$ while in the second we have set $\delta = 0.1$. The first value of δ implies a quasi-diagonal matrix, i.e. a system far from the transition, in which each stock is governed by its own dynamic. Differently, the second value of δ populates the off-diagonal part of $\mathbf{J}$ with elements of higher value, which implies that variables are no longer independent and that diffusion processes like herding behaviors dominate the dynamic of the system. This second case postulates a system near the transition phase.

Figure 10 shows the average dynamic of $\mathbf{Y}$ and $\mathbf{Z}$ as long as $P \to P_c$. This result has been obtained by simulating the dataset 100000 times and initializing, at each time step, $\mathbf{J}^*$ and $\hat{\mathbf{J}}$ with different randomly and uniformly distributed values. It is worth to notice that a low value of δ, which implies a quasi-diagonal Jacobian, produces a dominant eigenvalue (reported in the tag of the upper left panel) that is lower than the case in which $\mathbf{J}$ becomes more indecomposable (bottom left panel). The reduced decomposability of $\mathbf{J}$ translates in a structure approaching the transition (the value of $|\lambda_1|$ approaches to 1). Secondly, it is worth noticing how I^{AC} changes when δ varies as well. When the system approaches the transition point, I^{AC} takes a higher value. Figure 11 reports the histogram produced from the different simulations. In Figure 11 we can better observe how the values of I^{AC} increase as long as δ increases, thus as long as the system approaches a critical point. The distribution of I^{AC} becomes more skewed and also the average value of I^{AC}, depicted by the dashed red line, grows. This confirms our previously illustrated intuition about the connection between the decomposability of the Jacobian, near and far from the transition point, and the statistical characteristics of the originated time series captured by the indicator I^{AC}.

Additionally we inspect how, empirically, the decomposability degree is related with the early warning indicator we have proposed. Since we have no knowledge about the functional form of the equations describing the evolution of the stock markets, we can not compute the Jacobian matrix of such system. Therefore, we are forced to link the number of blocks of the correlation matrix of the empirical returns (used as a proxy of the decomposability) with the value of the LTM. Our aim is to show that the LTM anticipates stages of low demposability of the correlation matrix that are, in turn, linked to periods of financial distress and high systemic risk. We proceed as follow: we first compute the correlation matrix between stock returns considering

Figure 10: **Synthetic data dynamics.** Average dynamic of $\mathbf{Y}$ and $\mathbf{Z}$ far and near the transition point. In particular, the upper panels highlights a system far from the transition (as also indicated by the value assumed by $|\lambda_1|$) while the lower panels show the system dynamics near the transition point. The left panels depict the series of $\mathbf{Y}$ while the right ones concerns the series of $\mathbf{Z}$. In the sub-plots titles we have also inserted the average values of $|\lambda_1|$ and I^{AC}. Notice that the more indecomposable the Jacobian matrix is (the higher the value of δ), the closer to the transition point the system is, and the higher the value assumed by I^{AC}.

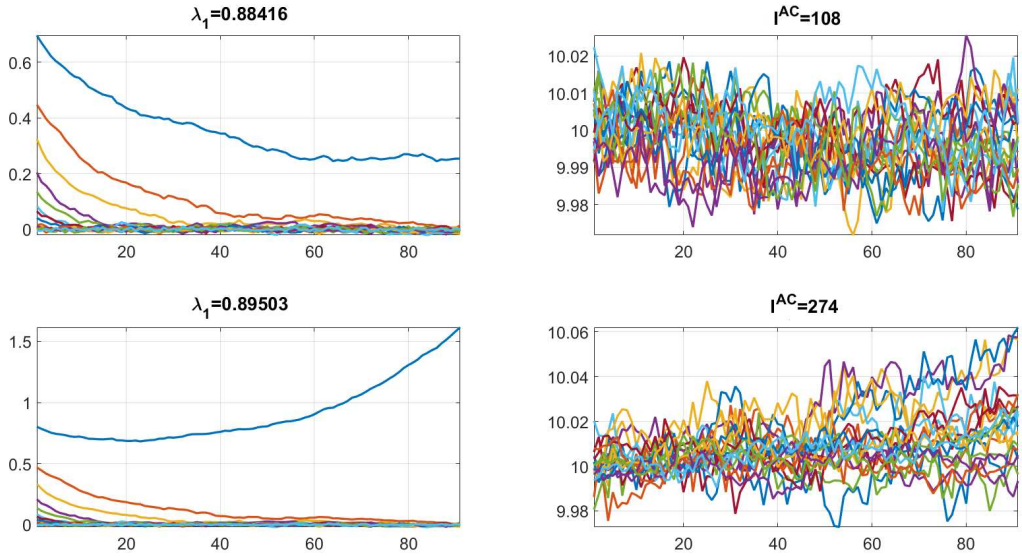

Figure 11: **Histogram of I^{AC} for different values of δ:** the left panel regards the distribution of I^{AC} obtained for $\delta = 0.01$ while the right panel shows the distribution of I^{AC} for $\delta = 0.1$. Near the transition phase, the distribution of I^{AC} becomes more skewed and the average value of I^{AC} (red dashed line) increases.

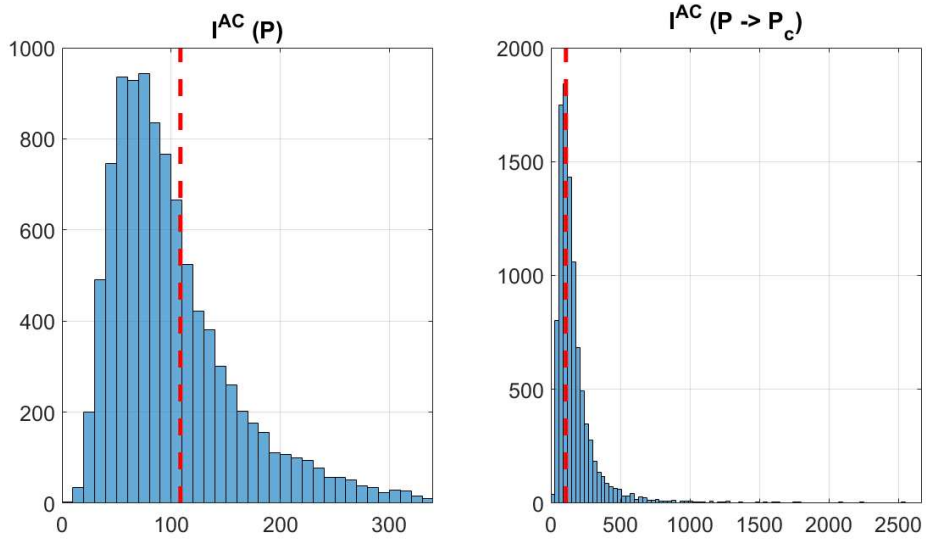

the same moving windows adopted for the extraction of the LTM; secondly, we set to zero the values of the correlations associated with a p-value less than 0.01; thirdly the symmetric reverse Cuthill-McKee ordering is applied to the correlation matrix. In so doing, we have its nonzero

elements closer to the diagonal and we obtain a block diagonal correlation matrix that reveals the number of connected components of the graph. Finally, the number of blocks is computed and a cross-correlation analysis between the LTM values and the reciprocal of the number of blocks is performed. Since a lower number of blocks indicates a higher indecomposability, and accordingly a higher likelihood of a systemic crisis, we expect its reciprocal to be positively related to the LTM values. Moreover we await the LTM anticipates the path of the number of blocks. The cross-correlation is thus performed to test these hypotheses. The cross-correlation function (ccf) of the two series is the product-moment correlation as function of the lag between the series:

$$ccf_{nb,ltm}(k) = \frac{c_{nb,ltm}(k)}{\sqrt{c_{nb,nb}(0)\, c_{ltm,ltm}(0)}}$$

where nb and ltm represent the reciprocal of the number of blocks and the leading temporal module respectively and $c(k)$ is the cross-covariance function (ccvf) defined as

$$c_{nb,ltm}(k) = \frac{1}{N}\sum_{t=1}^{N-k}\left(nb_t - \overline{nb}\right)\left(ltm_{t+k} - \overline{ltm}\right) \quad ; k = 0, 1, ..., (N-1)$$

$$c_{nb,ltm}(k) = \frac{1}{N}\sum_{t=1-k}^{N}\left(nb_t - \overline{bn}\right)\left(ltm_{t+k} - \overline{tlm}\right) \quad ; k = -1, ..., -(N-1)$$

where variables with upper bars indicate the average value. Figure 12 shows the cross-correlation

Figure 12: **Cross correlation values.** The three panels embody the cross-correlation values for 22 different time lags and leads for the STOXX North America 600 (left), the STOXX Europe 50 (central) and the STOXX Asia/Pacific 600 (right). The confidence bounds are ±0.036, ±0.033 and ±0.035, respectively.

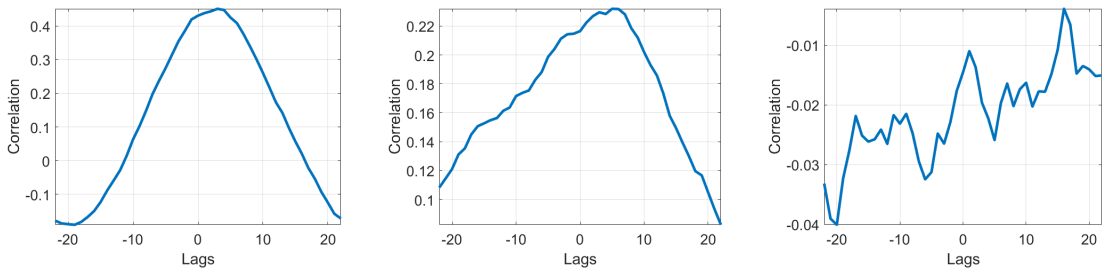

values for 22 different time lags and leads for the STOXX North America 600, the STOXX Europe 50 and the STOXX Asia/Pacific 600. The results are obtained by averaging the series obtained for the different moving windows. To emphasize the dynamics of the module size and to minimize noises, we have applied an average over a three-months moving window[11]. From

[11] Qualitatively, the results remain the same even without applying the moving average.

Figure 12 we can observe that the hypotheses are fulfilled for the STOXX North America 600 and, to a less extent, for the STOXX Europe 50. Indeed, for both the samples a positive cross-correlation peaks with a lag of one week, indicating that an above average value of the LTM is likely to lead a below average value of the number of blocks in the correlation matrix about one week later. For the STOXX Asia/Pacific 600, on the other hand, a negative correlation between the series exists, although results are not statistically significant.

C Non-parametric analysis

Early warning models are concerned with differentiating between vulnerable (i.e., pre-crisis and crisis periods) and tranquil phases, which forms a standard classification problem. Generally speaking, we are aiming for a model that separates vulnerable and tranquil classes and discriminates between them by estimating the probability of being in a vulnerable state. For backtesting, however, the time-series dimension needs to be taken into account when evaluating the predictive power. We conduct recursive real-time out-of-sample tests to assess the performance. This implies deriving a new model at each day using only information available up to that time point. By using information in a realistic manner, we test whether our measure has an ex-ante meaning for predicting crisis events. Following a standard evaluation framework for early-warning models, we aim at mimicking an ideal leading indicator $L \in \{0, 1\}$ that is a binary variable which takes value one during vulnerable periods and zero otherwise. We need a continuous measure indicating membership in a vulnerable state $p \in [0, 1]$, which is then turned into a binary prediction B that assume value one if p exceeds a specified threshold $\tau \in [0, 1]$ and zero otherwise. The correspondence between the prediction B and the ideal leading indicator L can be summarized into a contingency matrix, as described in Table 3.

To assess the predictive power of our indicator we calculate some standard measures from

Table 3: **Contingency matrix.**

		Actual Class	
		Pre-crisis period	Tranquil period
Predicted Class	Signal	Correct call *True Positive (TP)*	False alarm *False Positive (FP)*
	No Signal	Missed crisis *False Negative (FN)*	Correct silence *True Negative (TN)*

classification and machine learning literature, namely the area under the receiver operating characteristic (ROC) curve (AUROC) and the area under precision-recall (PR) curve (AUPR). ROC curves plot the false positive rate (FPR) against the true positive rate (TPR). To be more explicit:

$$FPR = \frac{FP}{FP + TN} \text{ and } TPR = \frac{TP}{TP + FN}$$

The PR curves plot precision (P) versus the recall (R), or, more explicitly:

$$P = \frac{TP}{TP + FP} \text{ and } R = \frac{TP}{TP + FN}$$

Precision is directly influenced by class (im)balance because of the false positive measure, whereas TPR only depends on positives. This is a drawback of ROC curves. PR curves are thus better to highlight the differences between models for highly imbalanced data sets where the cardinality of crisis events is much lower with respect to the number of tranquil periods.

D Value at Risk, Marginal Expected Shortfall and Absorption Ratio measures

An additional check involves the contrast between our measure and three well known indicator of risk, such as the Value at Risk (VaR) (see Jorion et al. (2007), Linsmeier and Pearson (2000)) the Marginal Expected Shortfall (MES) (see Oliviero et al. (2013)) and the Absorption Ratio (AR) (see Kritzman et al. (2010)). The VaR quantifies the maximum amount of loss over a certain time horizon and at a given confidence level. Assuming that profits and losses follow a normal distribution, the VaR can be computed by multiplying the z-score, at a certain confidence level, by the standard deviation of the returns. Moreover, all past returns are not assumed to carry the same weight. Accordingly, we apply an exponential weighted moving average (EWMA) method to assign different weights, and in particular we consider exponentially decreasing weights. The most recent returns have higher weights because they influence "today's" returns more heavily than returns further in the past (see Nieppola et al. (2009)). The formula for the EWMA variance over an estimation window of size w is:

$$\sigma_t^2 = \frac{1}{c}\sum_{i=1}^{w} \tau^{i-1} y_{t-1}^2 \tag{22}$$

where c s a normalizing constant, τ is the smoothing parameter set to 0.8 and y represents the STOXX indices. The VaR measure at the 0.95 confidence levels is:

$$VaR_t = -\sigma_t N^{-1}(0.05) \tag{23}$$

where N^{-1} is the inverse of a standardized Normal distribution.

Marginal Expected shortfall (MES) evaluates the expected return on a portfolio in the worst $q\%$ of cases. The MES is an alternative to the VaR for it is more sensitive to the shape of the tail of the loss distribution. The MES estimates the risk of an investment in a conservative way, giving more emphasis on the less profitable outcomes. The mathematical formulation is:

$$MES_t^q = \frac{1}{q}\int_0^q VaR_{y,t}\, dy \tag{24}$$

Finally, the AR represents the fraction of the total variance of a set of asset returns explained or absorbed by a fixed number of eigenvectors.

$$AR_t = \frac{\sum \sigma^2_{E_{i,t}}}{\sum \sigma^2_{A_{j,t}}} \tag{25}$$

where $\sigma^2_{E_{i,t}}$ is the variance of the i-th eigenvalues computed on the covariance matrix of returns of a given window w and $\sigma^2_{A_{j,t}}$ is the variance of the j-th asset. The AR aims at capturing how markets are unified or tightly coupled. When markets are tightly coupled, they become more fragile since negative shocks propagate more quickly and widely than when markets are loosely linked. A high value for the AR signals a high level of systemic risk, implying the sources of risk are more unified. Instead, a low AR indicates less systemic risk since the sources of risk are more disparate. Therefore, a high value of systemic risk is an indication of market fragility in the sense that a shock is more likely to quickly propagate when the sources of risk are tightly coupled.

E Empirical analysis: results on further datasets

In the next two subsection we shall show the application of our algorithm to two further datasets, namely the STOXX Europe 50 and the STOXX Asia/Pacific 600 indexes. As proceeded in the main text, we investigate whether the application of the technique we propose may provide information on the detection of EWSs.

E.1 Results on STOXX Europe 50

In order to disclose the LTM from the analysis of the STOXX Europe 50 dataset, Figure 13 emphasizes how, near a crisis stage, the LTM appears from the cross correlation matrix (top left panel) while its occurrence is not strong during business as usual phases (central left panel). As a consequence, our early warning indicators, namely I^{AC} and $I^{AC,STD}$, assume higher value around the 2008 financial crisis if compared to a tranquil phase, as the top and central right panels display. More precisely, we have computed the difference among the indexes of the stocks belonging to the LTM and the ones belonging to the other modules. This highlights the increasing magnitude of the proposed indicators when a period of financial distress takes place. Finally, the bottom panels of Figure 13 report the cumulative sum of the three indicators I^{AC}, I^{STD} and $I^{AC,STD}$ in the two different dates and higher values are observed in 2008.

Figure 14 shows the signals produced by the three alternative indicators that we consider. In particular, the red line refers to the original signals while the black lines are the correspondent smoothed versions. The series are plotted against the STOXX Europe 50 Index (in blue) to portray how the signals behave during different market phases. This analysis allows us to catch the most relevant market episodes of distress by comparing the dynamics of the indicators with the course of the market index.

The predictive performance of the three methodologies is tested through the ROC and the PR curves obtained for the different indicators, and reported in Figure 15. In the left panels we show the ROC curves while the right plots regard the PR curves. Broadly speaking, the performance of our indicator for the STOXX Europe 50 index exhibits a superior performance and a more informative signal with respect to the index proposed in Chen et al. (2012).

Figure 16 provides a broader view about the consistency of the results. The figure reports the AUROC values for all the different moving windows w where we also consider varying time steps for the leading indicator L. As expected, all the methods provide better EWSs in proximity of

Figure 13: **LTM and early warning indicators in different market phases.** The correlation matrix among stock returns together with the LTM is displayed for two different market phases, a distress (upper) and a business as usual (central) phase. From the plot clearly emerges the increased correlation among LTM stocks during a financial crisis. Moreover, the right panels show the percentage difference of the early warning indicators when computed on the LTM stocks or on the other modules. This difference increases during distress stages highlighting the importance of the LTM. The bottom panel reports the value of I^{AC}, I^{STD} and $I^{AC,STD}$ in 2008 and 2014. As expected the early warning indicators are higher in 2008.

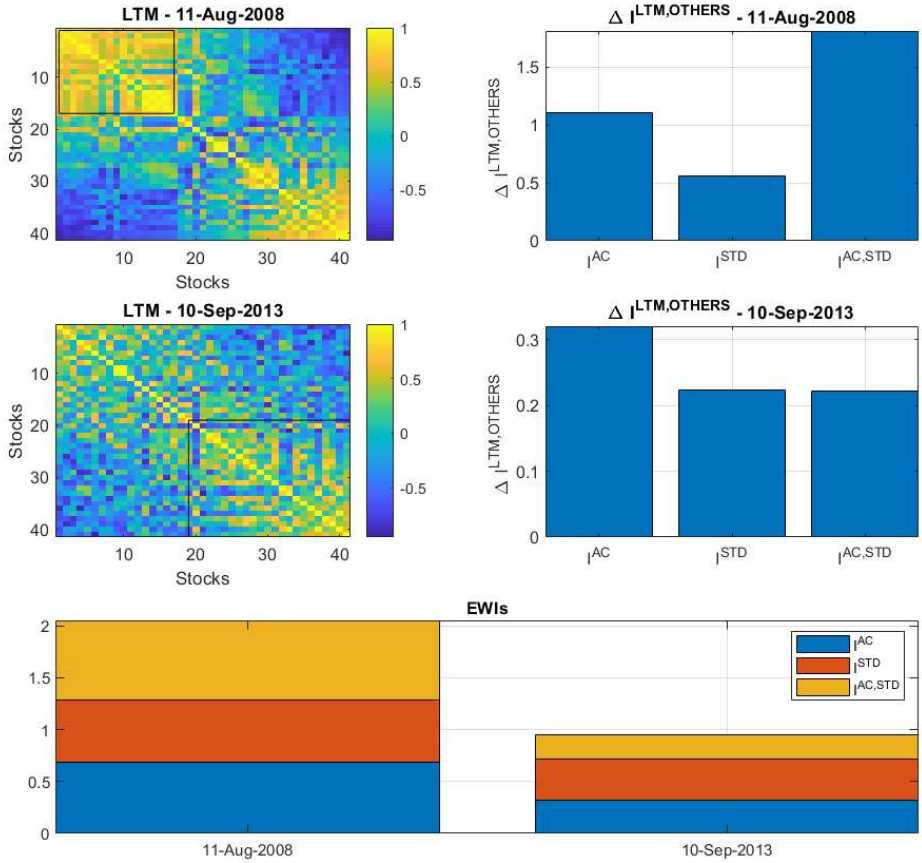

crisis periods, while the AUROC decrease as long as we want to anticipate a market crash with a wider time horizon. Moreover, this picture provides evidence that our method, together with the mixed signal, outperforms the indicator of Chen et al. (2012). Finally, the figure reveals that the AUROC of the smoothed index I_t^{AC} is, on average, the highest and that, for the -4% crisis scenario, it takes values around the 90% up to 10 days forward and around 75% up to 20 days forward.

The robustness of the previous findings is checked with respect to changes in the value of the parameter x. In Figure 17 and in Table 4 we show the average AUROC values obtained by letting the parameter x vary from 100% to 40%. Each bar represents the AUROC obtained by

Figure 14: **Early warning indicators patterns and the STOXX Europe 50 aggregate index dynamics.** The three panels represent the original early warning indicators (red), their smoothed version (black) and the STOXX Europe 50 aggregate index (blue). The upper panel refers to the indicator produced by using either the autocovariance or the standard deviation $I_t^{AC,STD}$ together with the PCC. The central panel encompasses our indicator I_t^{AC} which, beside PCC, takes into account only the autocovariance. The lower panel refers to the original index I_t^{STD} proposed by Chen et al. (2012).

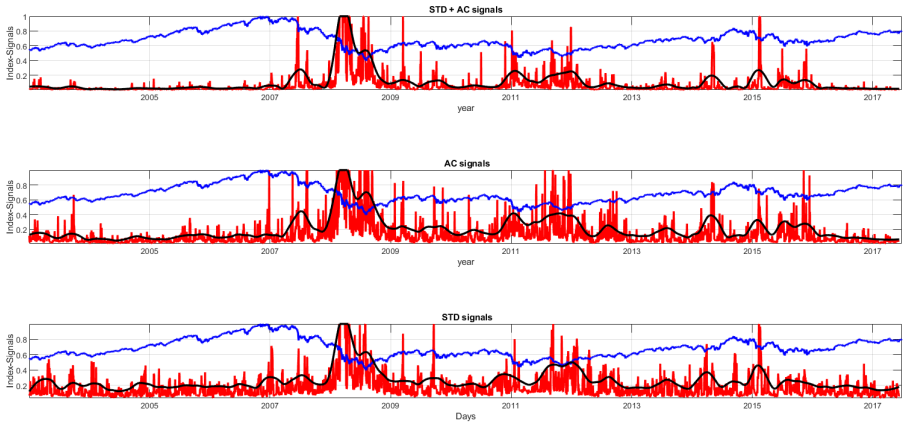

averaging the results of all the different moving windows (and of all the different values of the leading indicator L for the -4% crisis scenario) for a particular x.

From all the plots, it clearly emerges that our proposed technique and the mixed signal $I_t^{AC,STD}$ produce similar results and, depending on x and the type of scenarios, the former can be slightly better than the latter, but both overcome the indicator I_t^{STD}.

As a further check, we have compared the AUROC generated by I_t^{AC} with the ones derived from the other risk measures, i.e. VaR, MES and AR. Figure 18 reveals that our methodology generate superior performances in crisis signaling, with the only exception of the VaR in the -4% crisis scenario where the two methodologies perform equally.

E.2 Policy evaluations

Following the general line of the main text, in Table 5 we report the results obtained by applying the method developed by Sarlin (2013) to the indicator I_t^{AC}.

We report the results for the -3% crisis scenario, averaged along different moving windows. Results are in line with the discussion of the main text about the outcomes obtained for the United States and Canada.

Finally, the estimated distress levels obtained by the application of the HMM are presented in

Figure 15: **ROC and PR curves for the two crisis scenarios.** The left panels represent the ROC curves while the right plots encompass the PR curves. The upper panels refer to the -4% crisis scenario while the bottom ones describe the results related to the -3% case. In each plot we report the results obtained using either the original signals or the smoothed ones (SM). In particular, the label STD refers to I_t^{STD}, AC denotes our early warning indicator I_t^{AC} and finally STD+AC refers to the mixed signal $I_t^{AC,STD}$.

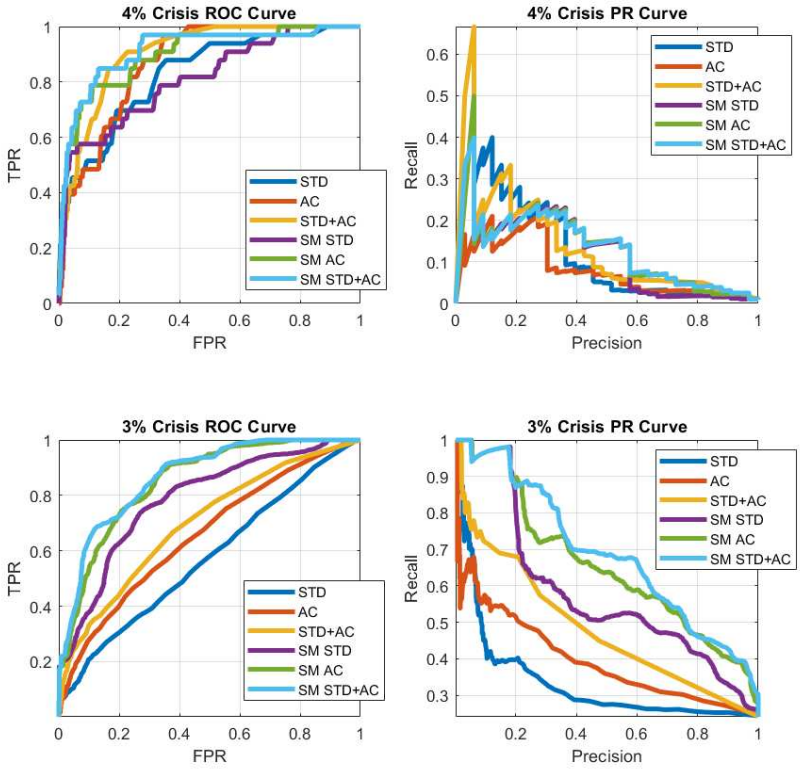

Figure 19. The estimation shows an increase in the level of distress, reaching a peak with the 2009 global financial crisis. The degree of distress reverts to a medium state in the subsequent few years while it takes another peak in correspondence to the 2011 European Sovereign debt crisis.

Figure 16: **AUROC values for the two crisis scenarios and for different moving windows.** Each plot represents the AUROC obtained by varying the moving window w used to compute the correlation coefficients. The background colors refer to the AUROC values related to the -4% crisis scenario in which, beside the different windows, we also consider varying time steps for the leading indicator L. L takes value 1 gradually, day by day, up to one month behind. The front line represents the AUROC for the -3% case where we consider the whole month for the leading indicator L. The upper panels represent the original indicators while the bottom ones encompass the results obtained for the smoothed indicators. The different columns represent the results obtained for, I_t^{STD} , I_t^{AC} and $I_t^{AC,STD}$ respectively.

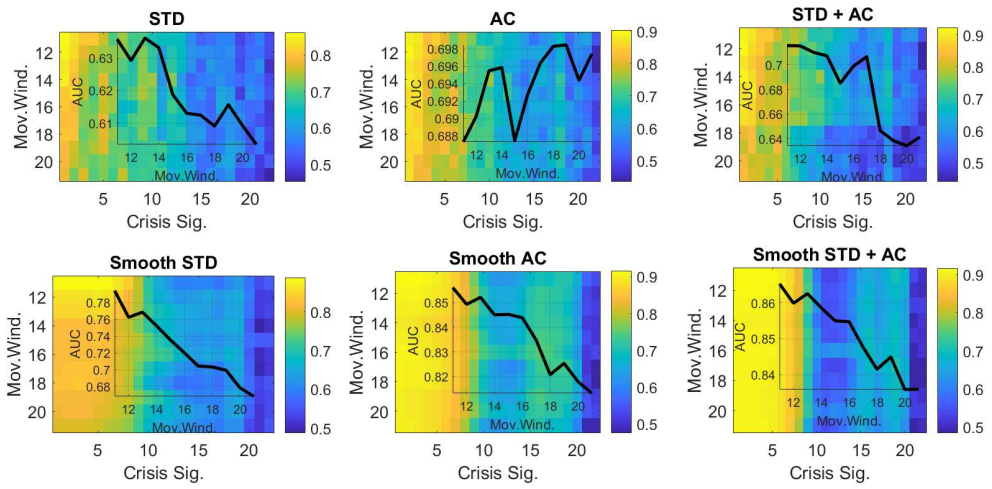

Figure 17: **Average AUROC for different values of the parameter x defining the percentage of stocks with the highest autocovariance (standard deviation) used for the clustering procedure.** Each plot represents the average AUROC obtained by varying the parameter x used to select the financial instruments with the highest autocovariance in the case of I_t^{AC} or standard deviation for I_t^{STD}. The parameter x varies from 100% to 40%. The upper panels refer to the -4% crisis scenario while the bottom ones describe the results related to the -3% case. The left plots encompass the results obtained by employing the original signals while the two plots on the right refer to the smoothed case.

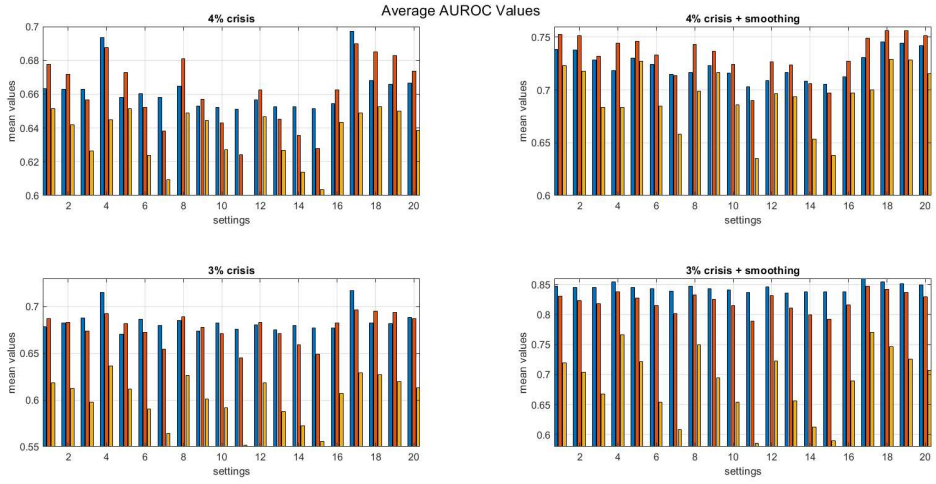

Table 4: **Average AUROC for different setting of the percentage of stocks with the highest auto-covariance (standard deviation) used for the clustering procedure.** The table represents the average AUROC obtained by modifying the parameter x used to select the financial instruments with the highest auto-covariance for I_t^{AC}, or standard deviation for I_t^{STD}. The parameter x varies from 100% to 40%. The first three columns refer to the -4% crisis scenario for $I_t^{AC,STD}$, I_t^{AC} and I_t^{STD} respectively. Columns from four to six refer to the -4% crisis scenario and to the smoothed (SM) indicators. Columns from seven to nine refer to the -3% scenario and the last three columns encompass the AUROC values of the smoothed (SM) indicators for the -3% crisis scenario.

4% Std + Ac	4% Ac	4% Std	4%-SM Std + Ac	4%-SM Ac	4%-SM Std	3% Std + Ac	3% Ac	3% Std	3%-SM Std + Ac	3%-SM Ac	3%-SM Std
0.6631	0.6776	0.6514	0.7386	0.7527	0.7232	0.6784	0.6868	0.6181	0.8467	0.8300	0.7199
0.6630	0.6717	0.6419	0.7376	0.7512	0.7179	0.6820	0.6831	0.6121	0.8448	0.8227	0.7034
0.6631	0.6566	0.6262	0.7285	0.7319	0.6837	0.6875	0.6738	0.5974	0.8447	0.8180	0.6678
0.6935	0.6878	0.6450	0.7183	0.7444	0.6836	0.7153	0.6926	0.6365	0.8546	0.8375	0.7658
0.6580	0.6727	0.6515	0.7302	0.7463	0.7274	0.6701	0.6816	0.6116	0.8445	0.8277	0.7213
0.6605	0.6522	0.6239	0.7242	0.7330	0.6846	0.6862	0.6723	0.5906	0.8425	0.8149	0.6538
0.6582	0.6382	0.6093	0.7148	0.7139	0.6579	0.6799	0.6543	0.5641	0.8387	0.8016	0.6086
0.6648	0.6809	0.6487	0.7164	0.7432	0.6991	0.6847	0.6891	0.6263	0.8475	0.8328	0.7492
0.6530	0.6569	0.6445	0.7234	0.7368	0.7168	0.6738	0.6777	0.6007	0.8424	0.8249	0.6945
0.6523	0.6431	0.6272	0.7157	0.7240	0.6860	0.6824	0.6711	0.5915	0.8411	0.8148	0.6538
0.6512	0.6242	0.5996	0.7030	0.6899	0.6354	0.6756	0.6453	0.5518	0.8362	0.7887	0.5855
0.6566	0.6626	0.6466	0.7089	0.7267	0.6968	0.6805	0.6830	0.6183	0.8455	0.8310	0.7222
0.6526	0.6453	0.6266	0.7165	0.7235	0.6936	0.6751	0.6709	0.5875	0.8359	0.8109	0.6564
0.6526	0.6356	0.6137	0.7082	0.7058	0.6534	0.6797	0.6588	0.5722	0.8373	0.7997	0.6128
0.6514	0.6280	0.6037	0.7056	0.6973	0.6380	0.6773	0.6490	0.5557	0.8379	0.7924	0.5897
0.6545	0.6626	0.6434	0.7126	0.7273	0.6973	0.6773	0.6823	0.6071	0.8379	0.8155	0.6896
0.6973	0.6900	0.6491	0.7306	0.7493	0.6999	0.7167	0.6966	0.6289	0.8596	0.8467	0.7703
0.6681	0.6852	0.6525	0.7455	0.7560	0.7288	0.6823	0.6951	0.6270	0.8540	0.8419	0.7461
0.6660	0.6827	0.6502	0.7444	0.7563	0.7286	0.6817	0.6940	0.6196	0.8511	0.8367	0.7261
0.6668	0.6736	0.6386	0.7418	0.7517	0.7155	0.6886	0.6869	0.6129	0.8495	0.8294	0.7074

Figure 18: **AUROC comparison.** The bars represent the average AUROC obtained by the VaR methodology, the MES and the AR along with the AUROC obtained with our indicator I_t^{AC} for the -4% and -3% crisis scenarios, and for the original and the smoothed (SM) indicators.

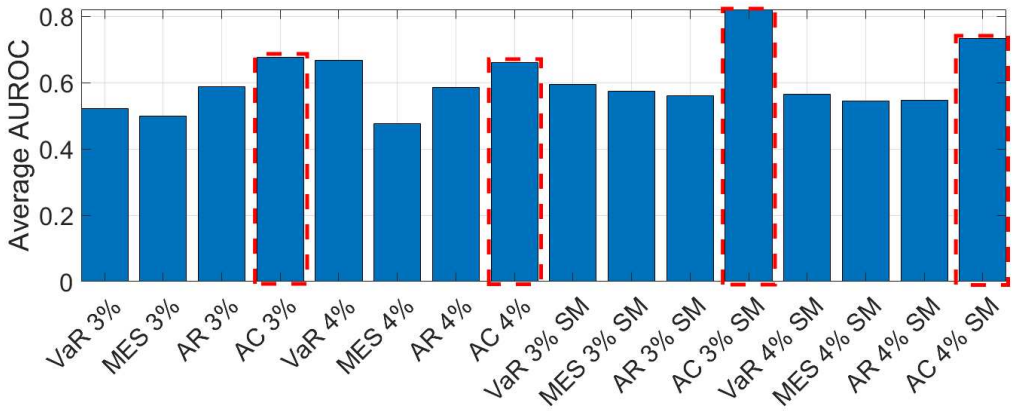

F Results on STOXX Asia/Pacific 600

The application of our EWS is tested also on the STOXX Asia/Pacific 600 market index, following the same analysis that has been carried on before. Accordingly, we start by showing the arising of the LTM in Figure 20 on the occasion of particular market event, as a financial crisis. In fact, the LTM appears from the cross correlation matrix (top left panel) while its occurrence is not strong during business as usual phases (central left panel). As a consequence, I^{AC} and $I^{AC,STD}$ assume higher value around the 2008 financial crisis if compared to a tranquil phase, as the top and central right panels display. More precisely, we have computed the

Table 5: **Policy Analysis.** We report, for different measures of preference (μ), the absolute usefulness (Abs. Usef.), the relative usefulness (Rel. Usef.) and the optimal threshold (Thresh.) for different moving windows (MW), 10 days, 15 days and 20 days. Results apply to the -3% crisis scenario.

μ	Abs. Usef. MW-10d	Rel. Usef. MW-10d	Thresh. MW-10d	Abs. Usef. MW-15d	Rel. Usef. MW-15d	Thresh. MW-15d	Abs. Usef. MW-20d	Rel. Usef. MW-20d	Thresh. MW-20d
0.0000	-0.0001	NaN	0.6932	-0.0002	NaN	0.7681	0.0000	NaN	0.3173
0.1000	0.0000	0.0011	0.6598	-0.0001	-0.0044	0.7681	0.0001	0.0054	0.3102
0.2000	0.0003	0.0072	0.4050	-0.0001	-0.0012	0.7368	0.0004	0.0082	0.2256
0.3000	0.0015	0.0202	0.2586	0.0002	0.0025	0.5155	0.0009	0.0126	0.1480
0.4000	0.0038	0.0390	0.1748	0.0024	0.0250	0.1135	0.0020	0.0206	0.0915
0.5000	0.0077	0.0635	0.1408	0.0061	0.0504	0.0973	0.0057	0.0471	0.0410
0.6000	0.0139	0.0964	0.0890	0.0121	0.0836	0.0675	0.0129	0.0888	0.0270
0.7000	0.0279	0.1653	0.0481	0.0282	0.1667	0.0271	0.0292	0.1726	0.0138
0.8000	0.0265	0.1748	0.0155	0.0260	0.1713	0.0113	0.0275	0.1811	0.0057
0.9000	0.0022	0.0296	0.0056	0.0020	0.0269	0.0036	0.0019	0.0255	0.0022
1.0000	0.0000	NaN	0.0010	0.0000	NaN	0.0010	0.0000	NaN	0.0010

Figure 19: **Discretization of the signal I_t^{AC} obtained through a Hidden Markov Model.** The figure presents the three states obtained by the discretization of the original signal I_t^{AC}. The blue bars, ranging from the lightest to the darkest, represent the low (cyan), medium (light blue) and high (dark blue) level of the system's distress while the red line denotes the STOXX Europe 50 index.

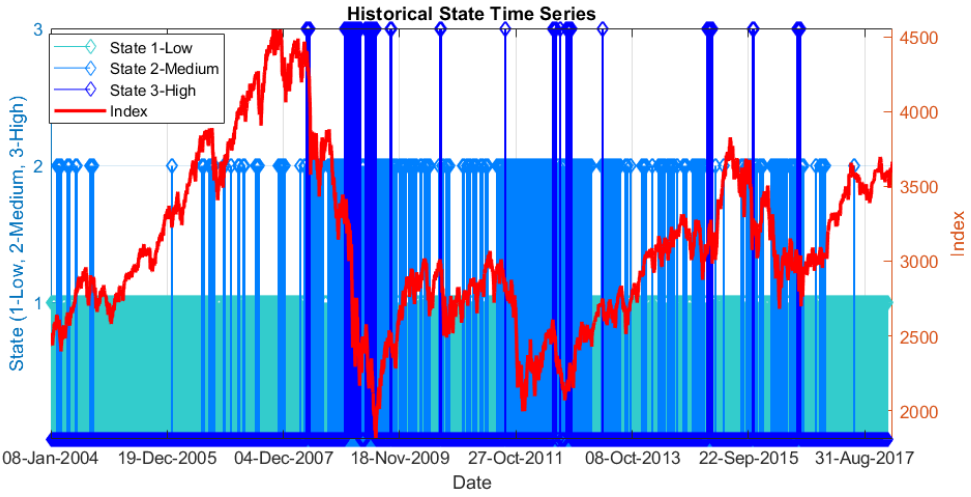

difference between the indexes of the stocks belonging to the LTM and the ones belonging to the other modules. This highlights the increasing magnitude of the proposed indicators when dealing with a period of financial distress. Finally, the bottom panels of Figure 20 accounts for the cumulative sum of the three indicators I^{AC}, I^{STD} and $I^{AC,STD}$ in the two different dates, and in 2008 we appraise higher values. The dynamics of the EWSs are reported in Figure 21, which displays I_t^{STD}, $I_t^{AC,STD}$ and I_t^{AC} along with the course of the market index STOXX Asia/Pacific 600 Index (blue). In particular the red lines refers to the raw indicators while the black lines are the corresponding smoothed versions.

The prediction performance of our EWS is shown in Figure 22 which portrays the ROC (left panels) and the PR (right panels) curves resulting from the different signals. As for the other datasets, in the -4% crisis scenario all the methodologies produce curves closer to the left-hand border and to the top border of the plotting space with respect to the -3% case. Again, it is plain that our method outperforms the index of Chen et al. (2012). Figure 23 shows the AUROC

Figure 20: **LTM and early warning indicators in different market phases.** The stock returns correlation matrix and the LTM are displayed for a distress (upper panels) phase and a business as usual (central panels) phase. From the plots, it clearly emerges the increased correlation among LTM stocks during a financial crisis. Moreover the right panels show the percentage difference of the early warning indicators when computed on the LTM stocks or on the other modules. This difference increases during distress stages, highlighting the importance of the LTM. The bottom panel reports the value of I^{AC}, I^{STD} and $I^{AC,STD}$ in 2008 and 2014. As expected, the early warning indicators assume higher values in 2008.

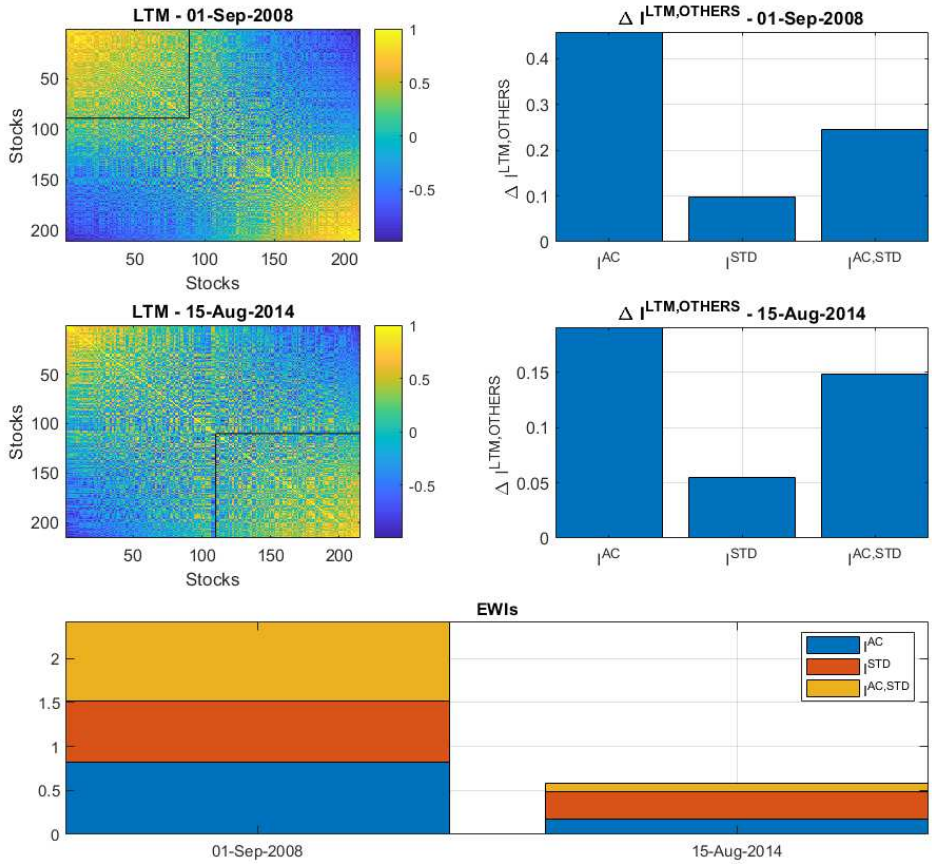

values for all the different moving windows w where varying time steps for the leading indicator L are also considered. Here, differently from the other two datasets, the indicators perform worse. Nonetheless, the methodology of Chen et al. (2012) generates the lowest AUROC values even if, similarly to the other two indicators, for the -4% crisis scenario, it takes values around 80% up to a week prior to the crisis. Moreover $I_t^{AC,STD}$ results to be the best indicator by producing AUROC values near 60% up to 20 days.

Figure 24 and Table 6 show the average AUROC values obtained by letting the parameter x vary from 100% to 40% as a robustness check. Each bar represents the AUROC obtained by averaging the results of all the different moving windows (and of all the different values of the

Figure 21: **Early warning indicators patterns and the STOXX Asia/Pacific 600 aggregate index dynamic.** The three panels represent the original early warning signals (red), the corresponding smoothed version (black) and the STOXX Asia/Pacific 600 aggregate index (blue). The upper panel relates to the signal produced by using autocovariance and standard deviation $I_t^{AC,STD}$, together with the PCC. The central panel encompasses the indicator I_t^{AC} while the lower panel refers to the signal I_t^{STD} proposed by Chen et al. (2012).

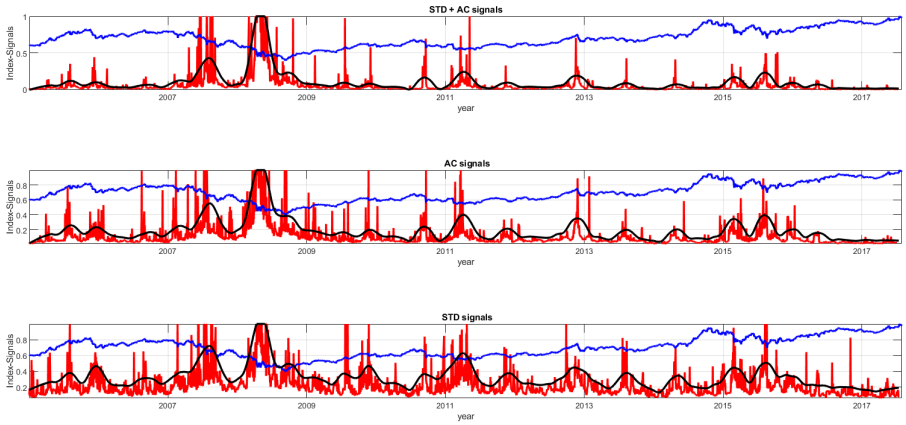

leading indicator L for the -4% crisis scenario) for a particular value of x. We observe that the mixed signal $I_t^{AC,STD}$ produces, on average, the best results but in few cases the I_t^{STD} index seems to outperform the others. Finally, we have compared the AUROC generated by I_t^{AC} with the ones resulting from the alternative risk measures, that is VaR, MES and AR. Figure 25 reveals that our methodology produces superior performances in crisis signaling except for the VaR in the -4% crisis scenario, where the two methodologies equally perform.

Figure 22: **ROC and PR curves for the two different crisis scenarios.** The left panels depict the ROC curves while the right plots highlight the PR curves. The upper panels refer to the -4% crisis scenario while the bottom ones describe the results related to the -3% case. In each plot we report the results of both the original indicators and the smoothed ones (SM). In particular, the label STD refers to I_t^{STD}, AC denotes our early warning indicator I_t^{AC} and finally STD+AC refers to the mixed signal $I_t^{AC,STD}$.

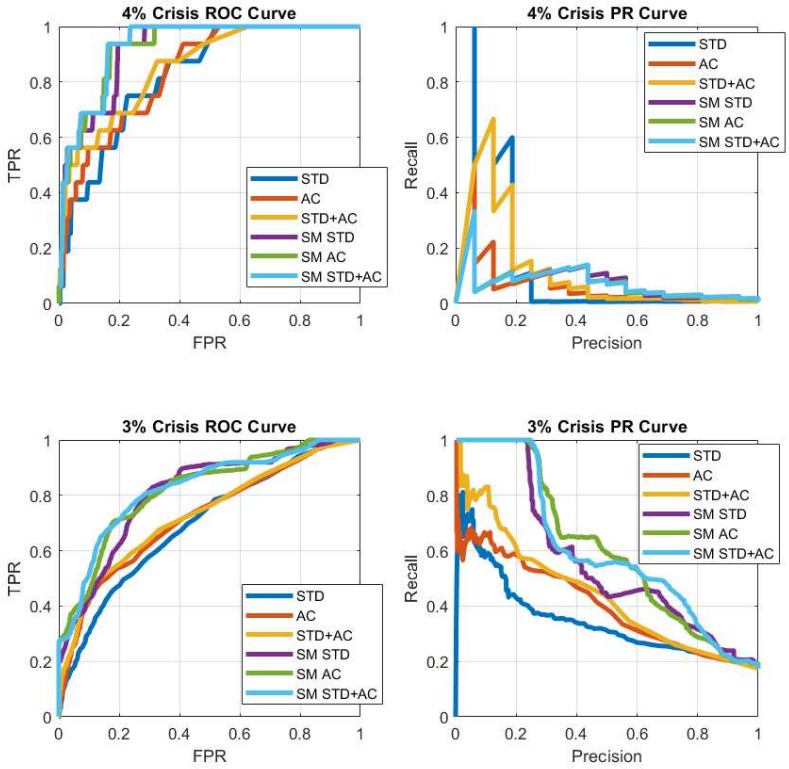

F.1 Policy evaluations

Finally, in Table 7 we report the results obtained by applying the method developed in Sarlin (2013) to the signal I_t^{AC}. Furthermore, the estimated distress levels obtained by the application of the HMM are presented in Figure 26.

As for the previous cases, also Asian financial markets have been hardly hit by the 2009 global financial crisis and, indirectly, by the 2011 European Sovereign debt crisis. Moreover, the figure also displays a high level of financial distress near 2013 due to the turmoil in some Asian emerging economies that has lead foreign investors to leave countries such as Indonesia, Malaysia and Thailand. Finally the Chinese currency devaluation has caused another peak of distress in 2015.

Figure 23: **AUROC for the two different crisis scenarios and for different moving windows.** Each plot represents the AUROC obtained by varying the moving window w used to compute the correlation coefficients. The background colors refer to the AUROC values related to the -4% crisis scenario in which, beside the different windows, we also consider varying time steps for the leading indicator L. L takes value 1 gradually, day by day, up to one month behind. The front line represents the AUROC for the -3% case where we consider the whole month for the leading indicator L. The upper panels represent the original series while the bottom ones encompass results obtained for the smoothed variables. The different columns represent the results obtained for I_t^{STD}, I_t^{AC} and $I_t^{AC,STD}$ respectively.

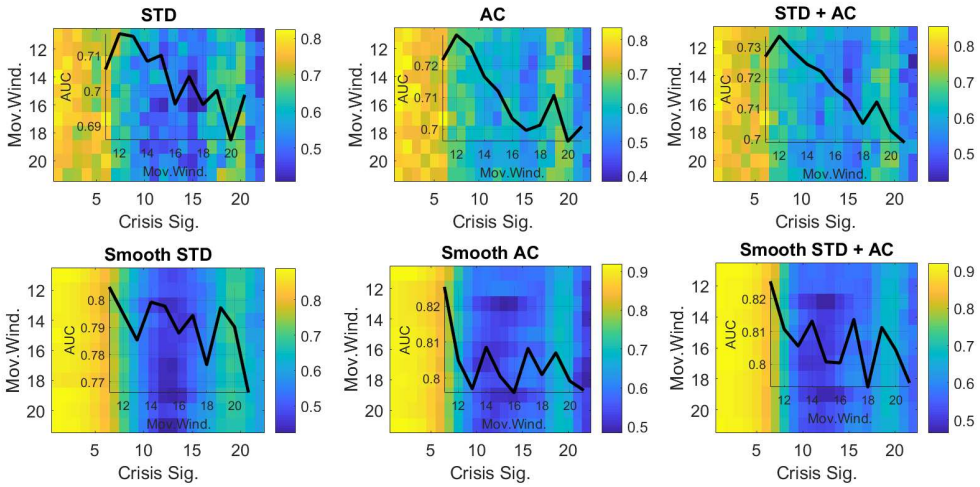

Figure 24: **Average AUROC for different setting of the parameter x defining the percentage of stocks with the highest autocovariance (standard deviation) used for the clustering procedure.** Each plot represents the average AUROC obtained on varying the parameter x used to choose the financial instruments with the highest autocovariance for I_t^{AC} or standard deviation for I_t^{STD}. The parameter x ranges from 100% to 40%. The upper panels refer to the -4% crisis scenario while the bottom ones describe the results in the -3% case. The left plots show the results obtained by employing the originals signals while the two plots on the right refer to the smoothed cases.

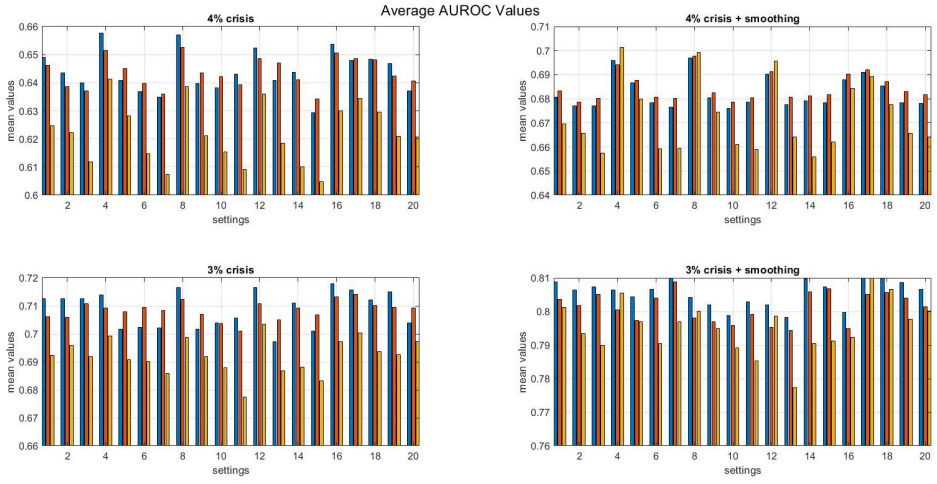

Tabel 6: **Average AUROC for different setting of the percentage of stocks with the highest autocovariance (standard deviation) used for the clustering procedure.** The table represents the average AUROC obtained by varying the parameter used to select the financial instruments with the highest autocovariance in the case of I_t^{AC} or standard deviation for I_t^{STD}. The parameter x varies from 100% to 40%. The first three columns deal with the -4% crisis scenario for $I_t^{AC,STD}$, I_t^{AC} and I_t^{STD} respectively. Columns from four to six refer to the -4% crisis scenario and to the smoothed (SM) indicators. Columns from seven to nine refer to the -3% scenario and the last three columns report the AUROC values for the -4% crisis scenario and to the smoothed (SM) indicators.

4% Std + Ac	4% Ac	4% Std	4%-SM Std + Ac	4%-SM Ac	4%-SM Std	3% Std + Ac	3% Ac	3% Std	3%-SM Std + Ac	3%-SM Ac	3%-SM Std
0.6490	0.6462	0.6248	0.6807	0.6832	0.6696	0.7126	0.7060	0.6923	0.8087	0.8037	0.8013
0.6434	0.6386	0.6222	0.6772	0.6787	0.6658	0.7125	0.7059	0.6958	0.8063	0.8018	0.7934
0.6399	0.6370	0.6119	0.6772	0.6803	0.6574	0.7126	0.7107	0.6920	0.8073	0.8051	0.7899
0.6576	0.6515	0.6412	0.6959	0.6940	0.7014	0.7139	0.7092	0.6992	0.8064	0.8004	0.8056
0.6409	0.6450	0.6282	0.6865	0.6876	0.6799	0.7016	0.7078	0.6907	0.8043	0.7973	0.7969
0.6368	0.6397	0.6146	0.6784	0.6808	0.6593	0.7023	0.7094	0.6901	0.8066	0.8040	0.7904
0.6348	0.6359	0.6073	0.6766	0.6801	0.6596	0.7021	0.7083	0.6859	0.8127	0.8088	0.7969
0.6571	0.6527	0.6387	0.6968	0.6977	0.6992	0.7166	0.7124	0.6988	0.8042	0.7980	0.8001
0.6397	0.6435	0.6212	0.6804	0.6824	0.6746	0.7017	0.7069	0.6920	0.8020	0.7969	0.7950
0.6381	0.6423	0.6154	0.6762	0.6786	0.6611	0.7039	0.7036	0.6879	0.7988	0.7957	0.7892
0.6430	0.6393	0.6093	0.6787	0.6803	0.6591	0.7057	0.7011	0.6775	0.8029	0.7992	0.7854
0.6524	0.6485	0.6359	0.6902	0.6912	0.6957	0.7166	0.7107	0.7034	0.8020	0.7954	0.7986
0.6409	0.6471	0.6184	0.6776	0.6808	0.6642	0.6973	0.7051	0.6868	0.7982	0.7944	0.7773
0.6437	0.6410	0.6101	0.6792	0.6812	0.6560	0.7109	0.7093	0.6881	0.8097	0.8058	0.7904
0.6294	0.6342	0.6047	0.6784	0.6816	0.6622	0.7010	0.7068	0.6833	0.8072	0.8068	0.7912
0.6537	0.6506	0.6299	0.6879	0.6904	0.6843	0.7179	0.7133	0.6973	0.7998	0.7948	0.7924
0.6479	0.6485	0.6345	0.6910	0.6920	0.6891	0.7157	0.7141	0.7004	0.8121	0.8050	0.8150
0.6483	0.6481	0.6297	0.6853	0.6870	0.6775	0.7121	0.7102	0.6937	0.8108	0.8056	0.8066
0.6468	0.6425	0.6209	0.6785	0.6829	0.6658	0.7149	0.7094	0.6926	0.8086	0.8040	0.7977
0.6372	0.6407	0.6207	0.6780	0.6816	0.6642	0.7039	0.7092	0.6971	0.8066	0.8013	0.8000

Figure 25: **AUROC comparison.** The bar represent the average AUROC obtained by the VaR methodology, the MES and the AR along with the AUROC obtained with our indicator I_t^{AC} for the -4% and -3% crisis scenarios, and for either the original indicators or the smoothed ones.

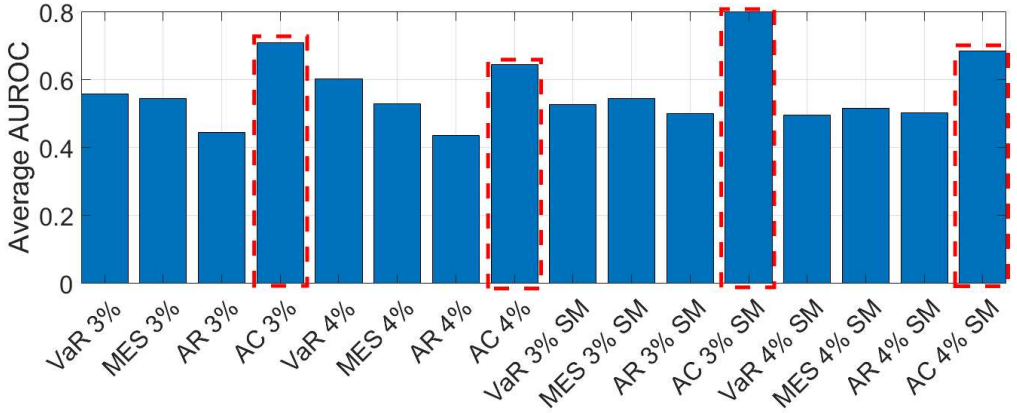

Table 7: **Policy Analysis.** We report, for different measures of preference μ, the absolute usefulness (Abs. Usef.), the relative usefulness (Rel. Usef.) and the optimal threshold (Thresh.) for different moving windows (MW), 10 days, 15 days and 20 days. Results refer to the -3% crisis scenario.

μ	Abs. Usef. MW-10d	Rel. Usef. MW-10d	Thresh. MW-10d	Abs. Usef. MW-15d	Rel. Usef. MW-15d	Thresh. MW-15d	Abs. Usef. MW-20d	Rel. Usef. MW-20d	Thresh. MW-20d
0.0000	-0.0001	NaN	0.4825	-0.0001	NaN	0.5256	-0.0000	NaN	0.5490
0.1000	-0.0000	-0.0028	0.4344	0.0001	0.0042	0.5219	0.0001	0.0042	0.5407
0.2000	0.0002	0.0055	0.2966	0.0003	0.0094	0.4327	0.0002	0.0065	0.4451
0.3000	0.0008	0.0157	0.0983	0.0009	0.0181	0.2742	0.0008	0.0159	0.2222
0.4000	0.0023	0.0338	0.0508	0.0023	0.0326	0.1751	0.0023	0.0322	0.0961
0.5000	0.0058	0.0671	0.0306	0.0050	0.0573	0.1047	0.0047	0.0537	0.0636
0.6000	0.0130	0.1245	0.0193	0.0111	0.1065	0.0597	0.0095	0.0905	0.0372
0.7000	0.0253	0.2079	0.0142	0.0231	0.1893	0.0412	0.0216	0.1768	0.0238
0.8000	0.0426	0.3064	0.0114	0.0419	0.3006	0.0288	0.0423	0.3031	0.0165
0.9000	0.0068	0.0818	0.0028	0.0063	0.0768	0.0051	0.0066	0.0804	0.0035
1.0000	0.0000	NaN	0.0010	0.0000	NaN	0.0010	0.0000	NaN	0.0010

Figure 26: **Discretization of the signal I_t^{AC} obtained through a Hidden Markov Model.** The figure presents the three states obtained by the discretization of the original indicator I_t^{AC}. The blue bars, ranging from the lightest to the darkest, represent the low (cyan), medium (light blue) and high (dark blue) level of the system distress while the red line represents the aggregate STOXX Asia/Pacific 600 aggregate index.

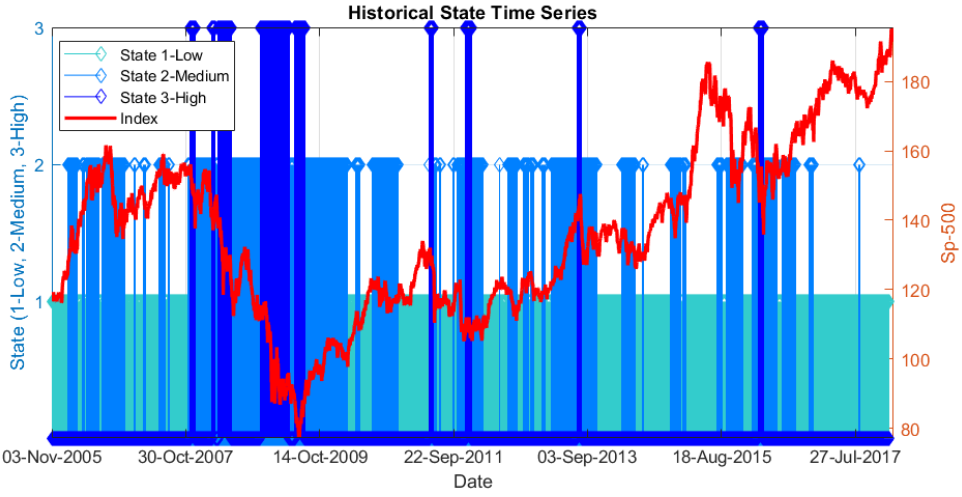

G AUPR results

In this Section we show the results of the robustness check as regards the AUPR values. The figures highlight how the findings modify to changes in the value of the parameter x representing the percentage of stocks selected for the clustering procedure. In Figures 27, 28 and 29 we present the average AUPR values obtained by letting the parameter x vary from 100% to 40%. Each bar represents the AUROC obtained by averaging the results of all the different moving windows (and of all the different values of the leading indicator L for the -4% crisis scenario) for a particular x. The corresponding values are reported in Tables 8-10.

Generally speaking, for AUPR, the mixed signal $I_t^{AC,STD}$ produces the best performance in all the three datasets, while our index I_t^{AC} follows with few exceptions, as in the case of the STOXX Europe 50 and the -4% crisis scenario where the I_t^{STD} comes second.

Figure 27: **Average AUPR for different setting of the parameter x defining the percentage of stocks with the highest autocovariance (standard deviation) for the STOXX North America 600.** Each plot represents the average AUPR obtained on varying the parameter x from 100% to 40% to select the financial instruments with the highest autocovariance in the case of I_t^{AC} or standard deviation for I_t^{STD}. The upper panels refer to the -4% crisis scenario while the bottom ones describe the results for the -3% case. The left plots detail the results obtained by employing the original indicators while the two plots on the right refers to the smoothed cases.

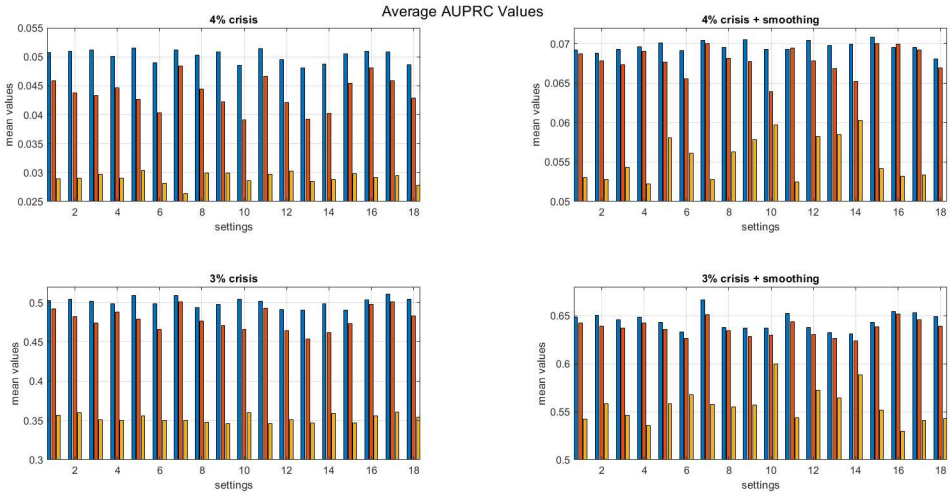

Table 8: **Average AUPR for different setting of the percentage of stocks with the highest autocovariance (standard deviation) for the STOXX North America 600.** The table represents the average AUPR obtained by varying the parameter used to select the financial instruments that possess the highest autocovariance for I_t^{AC} or standard deviation for I_t^{STD}. The parameter x varies from 100% to 40%. The first three columns refer to the -4% crisis scenario for $I_t^{AC,STD}$, I_t^{AC} and I_t^{STD} respectively. Columns from four to six refer to the -4% crisis scenario and to the smoothed indicators. Columns from seven to nine apply to the -3% scenario and the last three columns are devoted to the AUPR values for the -4% crisis scenario and to the smoothed indicators.

4% Std + Ac	4% Ac	4% Std	4%-SM Std + Ac	4%-SM Ac	4%-SM Std	3% Std + Ac	3% Ac	3% Std	3%-SM Std + Ac	3%-SM Ac	3%-SM Std
0.0508	0.0458	0.0289	0.0692	0.0688	0.0531	0.5028	0.4916	0.3567	0.5149	0.6422	0.3698
0.0509	0.0438	0.0290	0.0688	0.0678	0.0528	0.5044	0.4818	0.3596	0.5190	0.6388	0.3811
0.0512	0.0433	0.0297	0.0693	0.0673	0.0543	0.5017	0.4736	0.3510	0.5217	0.6372	0.3727
0.0501	0.0447	0.0291	0.0696	0.0690	0.0522	0.4988	0.4875	0.3498	0.5162	0.6421	0.3632
0.0515	0.0427	0.0304	0.0701	0.0677	0.0581	0.5087	0.4788	0.3556	0.5299	0.6358	0.3821
0.0490	0.0403	0.0281	0.0691	0.0656	0.0561	0.4987	0.4657	0.3500	0.5294	0.6265	0.3868
0.0512	0.0485	0.0264	0.0704	0.0700	0.0528	0.5088	0.5009	0.3500	0.5324	0.6508	0.3715
0.0503	0.0444	0.0299	0.0695	0.0682	0.0563	0.4936	0.4765	0.3479	0.5139	0.6342	0.3652
0.0509	0.0422	0.0299	0.0705	0.0677	0.0578	0.4975	0.4709	0.3463	0.5237	0.6283	0.3712
0.0485	0.0391	0.0286	0.0693	0.0639	0.0597	0.5039	0.4660	0.3599	0.5367	0.6300	0.4034
0.0514	0.0467	0.0297	0.0693	0.0694	0.0525	0.5016	0.4928	0.3457	0.5240	0.6435	0.3625
0.0496	0.0421	0.0302	0.0705	0.0678	0.0582	0.4909	0.4643	0.3511	0.5178	0.6303	0.3746
0.0481	0.0392	0.0285	0.0698	0.0668	0.0585	0.4906	0.4535	0.3470	0.5221	0.6263	0.3765
0.0487	0.0402	0.0288	0.0699	0.0652	0.0603	0.4985	0.4615	0.3587	0.5336	0.6237	0.4012
0.0506	0.0454	0.0298	0.0708	0.0700	0.0542	0.4900	0.4734	0.3468	0.5143	0.6386	0.3646
0.0510	0.0480	0.0292	0.0695	0.0699	0.0532	0.5037	0.4975	0.3556	0.5122	0.6519	0.3660
0.0508	0.0459	0.0295	0.0695	0.0692	0.0533	0.5106	0.5011	0.3604	0.5208	0.6455	0.3713
0.0487	0.0428	0.0278	0.0680	0.0669	0.0498	0.5041	0.4833	0.3545	0.5159	0.6389	0.3649

Figure 28: **Average AUPR for different setting of the parameter x defining the percentage of stocks with the highest autocovariance (standard deviation) for the STOXX Europe 50.** Each plot represents the average AUPR obtained by varying the parameter x, from 100% to 40%, used to select the financial instruments with the highest autocovariance for I_t^{AC} or standard deviation for I_t^{STD}. The upper panels refer to the -4% crisis scenario while the bottom ones describe the results related to the -3% case. The left plots gather the results obtained by employing the original indicators while the two plots on the right refers to the smoothed cases.

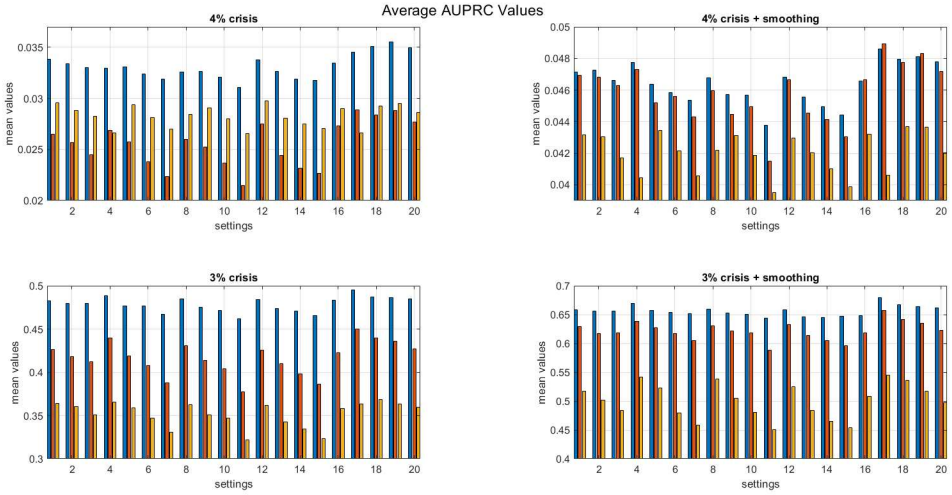

Table 9: **Average AUPR for different setting of the percentage of stocks with the highest autocovariance (standard deviation) for the STOXX Europe 50.** The table represents the average AUPR obtained by varying the parameter used to select the financial instruments with the highest autocovariance for I_t^{AC} or standard deviation for I_t^{STD}. The parameter x varies from 100% to 40%. The first three columns refer to the -4% crisis scenario for $I_t^{AC,STD}$, I_t^{AC} and I_t^{STD} respectively. Columns from four to six refer to the -4% crisis scenario and to the smoothed indicators. Columns from seven to nine refer to the -3% scenario and the last three columns encompass the AUPR values for the -4% crisis scenario and to the smoothed indicators.

4% Std + Ac	4% Ac	4% Std	4%-SM Std + Ac	4%-SM Ac	4%-SM Std	3% Std + Ac	3% Ac	3% Std	3%-SM Std + Ac	3%-SM Ac	3%-SM Std
0.0338	0.0265	0.0295	0.0471	0.0469	0.0431	0.4825	0.4261	0.3641	0.6581	0.6291	0.5175
0.0334	0.0257	0.0288	0.0473	0.0468	0.0430	0.4794	0.4182	0.3600	0.6557	0.6172	0.5018
0.0330	0.0245	0.0282	0.0466	0.0463	0.0417	0.4799	0.4119	0.3510	0.6565	0.6181	0.4835
0.0329	0.0269	0.0266	0.0477	0.0473	0.0405	0.4886	0.4397	0.3652	0.6697	0.6386	0.5412
0.0331	0.0258	0.0294	0.0464	0.0452	0.0434	0.4769	0.4186	0.3585	0.6567	0.6274	0.5223
0.0324	0.0238	0.0281	0.0458	0.0456	0.0421	0.4765	0.4081	0.3468	0.6534	0.6177	0.4794
0.0319	0.0223	0.0270	0.0454	0.0443	0.0406	0.4674	0.3875	0.3310	0.6512	0.6048	0.4578
0.0326	0.0260	0.0284	0.0468	0.0459	0.0422	0.4848	0.4305	0.3627	0.6595	0.6303	0.5386
0.0326	0.0252	0.0291	0.0457	0.0445	0.0431	0.4753	0.4139	0.3511	0.6524	0.6218	0.5054
0.0321	0.0237	0.0280	0.0457	0.0450	0.0419	0.4715	0.4038	0.3467	0.6508	0.6183	0.4809
0.0311	0.0215	0.0266	0.0438	0.0415	0.0395	0.4621	0.3775	0.3219	0.6442	0.5882	0.4509
0.0337	0.0275	0.0297	0.0468	0.0467	0.0430	0.4839	0.4256	0.3621	0.6582	0.6322	0.5253
0.0326	0.0244	0.0281	0.0456	0.0446	0.0420	0.4740	0.4097	0.3429	0.6466	0.6141	0.4834
0.0319	0.0232	0.0275	0.0449	0.0441	0.0410	0.4709	0.3980	0.3344	0.6447	0.6054	0.4647
0.0318	0.0227	0.0271	0.0444	0.0430	0.0399	0.4658	0.3860	0.3234	0.6472	0.5956	0.4543
0.0334	0.0273	0.0290	0.0466	0.0467	0.0432	0.4833	0.4229	0.3581	0.6483	0.6182	0.5078
0.0345	0.0289	0.0266	0.0486	0.0489	0.0406	0.4952	0.4503	0.3636	0.6794	0.6573	0.5445
0.0351	0.0284	0.0292	0.0479	0.0478	0.0437	0.4871	0.4398	0.3689	0.6667	0.6421	0.5361
0.0355	0.0288	0.0295	0.0481	0.0483	0.0437	0.4866	0.4362	0.3630	0.6644	0.6351	0.5169
0.0350	0.0277	0.0286	0.0478	0.0472	0.0420	0.4852	0.4269	0.3598	0.6622	0.6229	0.4969

Figure 29: **Average AUPR for different setting of the parameter x defining the percentage of stocks with the highest autocovariance (standard deviation) for the STOXX Asia/Pacific 600.** Each plot represents the average AUPRC obtained by varying the parameter x used to select the financial instruments with the highest autocovariance for I_t^{AC} or standard deviation for I_t^{STD} from 100% to 40%. The upper panels refer to the -4% crisis scenario while the bottom ones describe the results related to the -3% case. The left plots encompass results obtained by employing the original indicators while the two plots on the right refers to the smoothed cases.

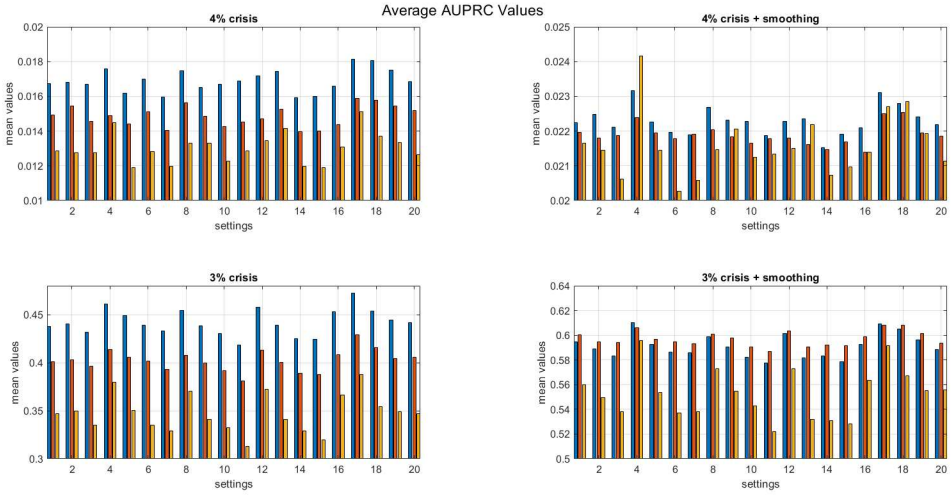

Table 10: **Average AUPR for different setting of the percentage of stocks with the highest autocovariance (standard deviation) for the STOXX Asia/Pacific 600.** The table represents the average AUPR obtained by varying the parameter used to select the financial instruments with the highest autocovariance for I_t^{AC} or standard deviation for I_t^{STD}. The parameter x varies from 100% to 40%. The first three columns refer to the -4% crisis scenario for $I_t^{AC,STD}$, I_t^{AC} and I_t^{STD} respectively. Columns from four to six refer to the -4% crisis scenario and to the smoothed indicators. Columns from seven to nine refer to the -3% scenario and the last three columns report the AUPR values for the -4% crisis scenario and to the smoothed indicators.

4% Std + Ac	4% Ac	4% Std	4%-SM Std + Ac	4%-SM Ac	4%-SM Std	3% Std + Ac	3% Ac	3% Std	3%-SM Std + Ac	3%-SM Ac	3%-SM Std
0.0167	0.0149	0.0129	0.0222	0.0220	0.0216	0.4379	0.4010	0.3470	0.5948	0.6001	0.5600
0.0168	0.0155	0.0127	0.0225	0.0218	0.0214	0.4403	0.4027	0.3494	0.5891	0.5944	0.5493
0.0167	0.0146	0.0127	0.0221	0.0219	0.0206	0.4317	0.3966	0.3353	0.5832	0.5939	0.5383
0.0176	0.0149	0.0145	0.0232	0.0224	0.0242	0.4612	0.4137	0.3799	0.6101	0.6060	0.5957
0.0162	0.0144	0.0119	0.0223	0.0220	0.0214	0.4492	0.4053	0.3504	0.5927	0.5969	0.5537
0.0170	0.0151	0.0128	0.0220	0.0218	0.0203	0.4388	0.4018	0.3351	0.5862	0.5949	0.5369
0.0160	0.0141	0.0120	0.0219	0.0219	0.0206	0.4333	0.3929	0.3287	0.5857	0.5933	0.5381
0.0175	0.0156	0.0133	0.0227	0.0220	0.0215	0.4540	0.4078	0.3704	0.5988	0.6011	0.5730
0.0165	0.0148	0.0133	0.0223	0.0218	0.0221	0.4384	0.3997	0.3412	0.5904	0.5975	0.5549
0.0167	0.0143	0.0123	0.0223	0.0216	0.0213	0.4302	0.3918	0.3326	0.5824	0.5903	0.5429
0.0169	0.0145	0.0129	0.0219	0.0218	0.0213	0.4187	0.3810	0.3131	0.5776	0.5869	0.5222
0.0172	0.0147	0.0135	0.0223	0.0218	0.0215	0.4575	0.4129	0.3725	0.6014	0.6033	0.5727
0.0174	0.0152	0.0142	0.0223	0.0216	0.0222	0.4388	0.4005	0.3411	0.5816	0.5904	0.5319
0.0159	0.0140	0.0120	0.0215	0.0215	0.0207	0.4252	0.3893	0.3291	0.5832	0.5919	0.5311
0.0160	0.0140	0.0119	0.0219	0.0217	0.0210	0.4241	0.3877	0.3199	0.5787	0.5918	0.5284
0.0166	0.0144	0.0131	0.0221	0.0214	0.0214	0.4530	0.4083	0.3662	0.5924	0.5990	0.5635
0.0181	0.0159	0.0151	0.0231	0.0225	0.0227	0.4725	0.4291	0.3880	0.6093	0.6080	0.5915
0.0180	0.0158	0.0137	0.0228	0.0225	0.0228	0.4536	0.4158	0.3541	0.6049	0.6083	0.5669
0.0175	0.0154	0.0133	0.0224	0.0219	0.0219	0.4445	0.4047	0.3492	0.5961	0.6013	0.5550
0.0169	0.0152	0.0127	0.0222	0.0219	0.0211	0.4418	0.4057	0.3469	0.5886	0.5934	0.5559

H Additional results

The efficacy of our crisis indicator is tested by mean of non parametric analysis and, in order to proceed in this sense, we need the definition of certain thresholds to characterize crisis events. We select two thresholds to indicate a financial distress period, namely a drop of at least 3% of the aggregate index returns and a drop of a 4% respectively. In both cases the selected values represent extreme events that lie in the first percentile of the returns distribution as Figure 30 shows. These thresholds have been used as a reference point for crisis occurrence along the empirical analysis.

In order to infer the possible crisis events we analyze the behavior of the indices' constituents. Our approach has disregarded the weight that the components have in the construction of the aggregate index. This is so to exclude the trivial case in which the constituents with the highest weights play the major role in determining the dynamics of our EWS. As a confirm, we have computed the average weight of the stocks in the LTM. We have then calculated the distribution of the averaged values across all the settings for I_t^{STD}, I_t^{AC} and $I_t^{AC,STD}$.

Figures 31-33 show the distributions of the stocks' weight inside the LTM for the STOXX North America 600, STOXX Europe 50 and STOXX Asia/Pacific 600 respectively, along with their mean values. From the figures, it clearly emerges how the LTM is not related to the weights that stocks carry on in the indices construction. On average, a LTM encompasses stocks that have a 0.1% weight for the STOXX North America 600 index and for the STOXX Asia/Pacific 600 index while the average for the STOXX Europe 50 index is higher (around 1.5%) due to the lower number of stocks composing this index. Moreover, from all the figures we notice that the weights distribution is more skewed than a Gaussian distribution. This finding applies to all the three financial markets.

Figure 30: **Returns distributions and first percentile indicating crisis thresholds.** The three panels represent the return distributions of the aggregate indices while the dashed red lines indicate the first percentile of the distributions. This threshold has been used as a reference point for crisis occurrence along the empirical analysis. In particular the left panel refers to the STOXX Europe 50, the central panel to the STOXX North America 600 and the right panel to the STOXX Asia/Pacific 600.

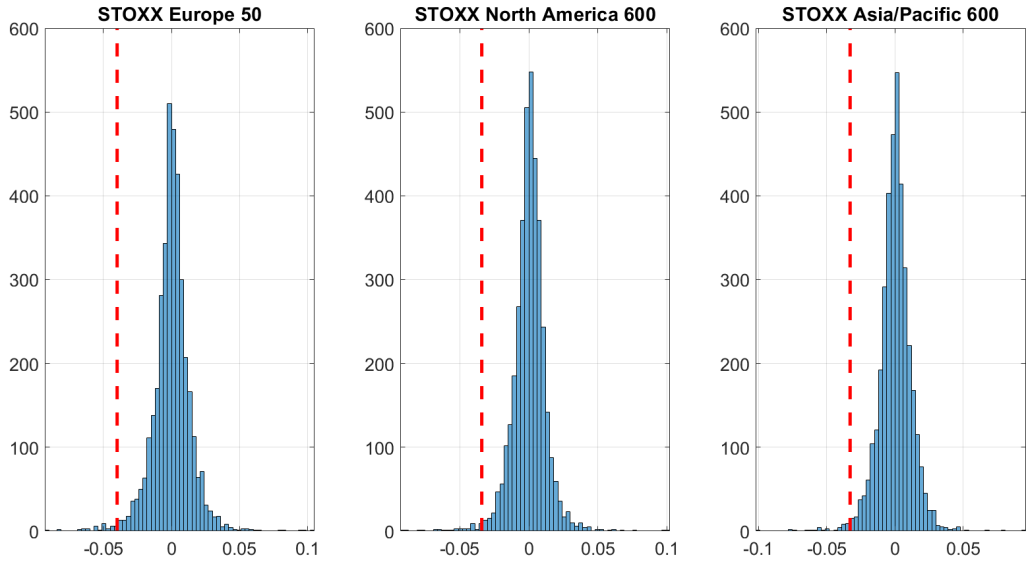

Figure 31: **Weights distributions of the stocks inside the LTM in STOXX North America 600.** The left panel represents the case of I_t^{STD}, the central panel encompasses the distribution of the stocks' weights into I_t^{AC} and the right panel refers to $I_t^{AC,STD}$. As the picture suggests, the LTM represents a fraction of shares that have on average a weight of 0.1% on the entire STOXX North America 600 index.

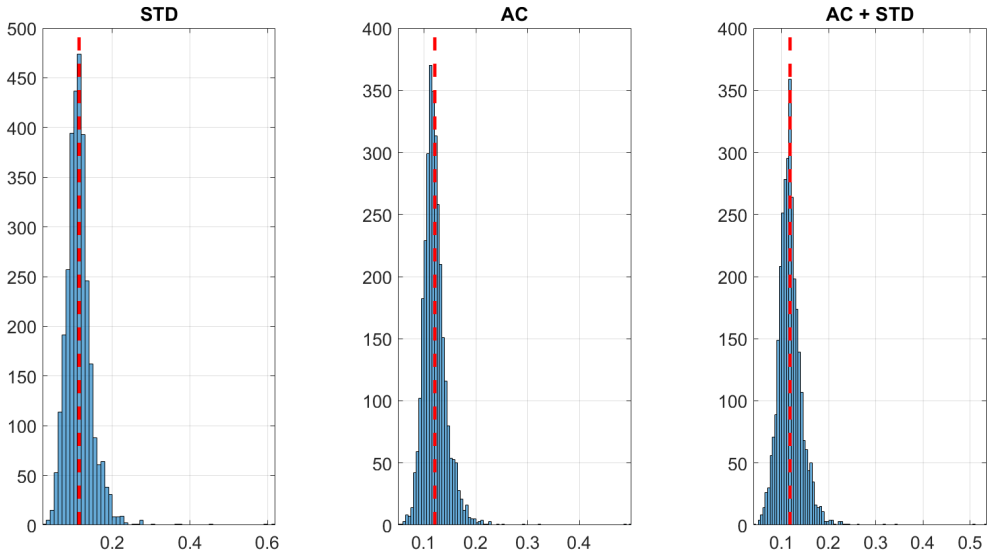

Figure 32: **Weights distribution of the stocks inside the LTM for the STOXX Europe 50 Index.** The left panel represents the case of I_t^{STD}, the central panel encompasses the distribution of the stocks' weights into I_t^{AC} and the right panel refers to $I_t^{AC,STD}$. The LTM includes stocks that have on average a weight of 1.5% within the STOXX Europe 50 Index.

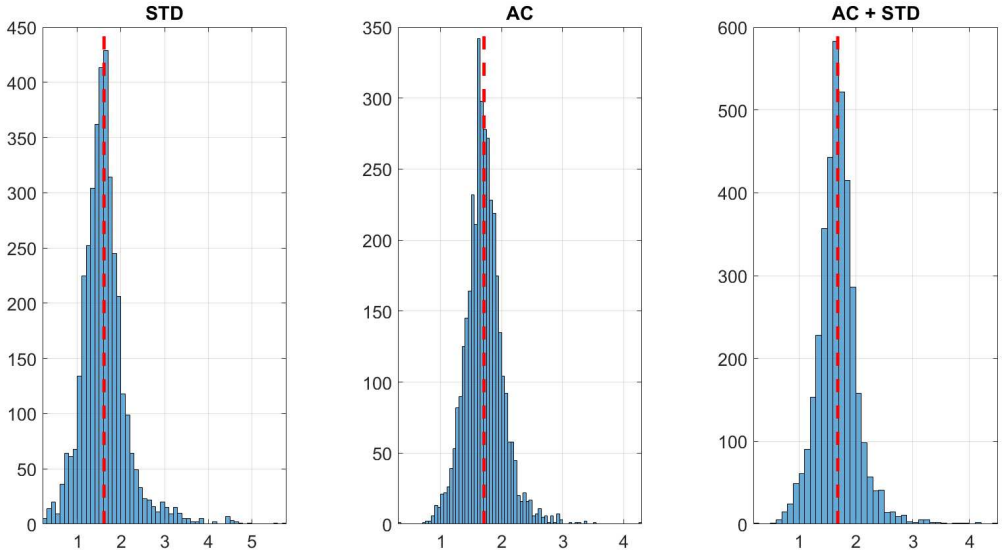

Figure 33: **Weights distribution of the stocks inside the LTM for the STOXX Asia/Pacific 600.** The left panel represents the case of I_t^{STD}, the central panel encompasses the distribution of the stocks' weights into I_t^{AC} and the right panel refers to $I_t^{AC,STD}$. The LTM groups stocks that have on average a weights of 0.1% within the STOXX Asia/Pacific 600 Index.